

Assessment of Chemical Conversion Coatings for the Protection of Aluminium Alloys

A Comparison of Alodine 1200 with Chromium-Free Conversion Coatings

A.M. Pereira, G. Pimenta

Instituto de Soldadura e Qualidade (ISQ), Oeiras, Portugal

B.D. Dunn

Product Assurance and Safety Department, ESA/ESTEC,
The Netherlands

Publication: Assessment of Chemical Conversion Coatings for the
Protection of Aluminium Alloys (ESA STM-276,
February 2008)

Editor: K. Fletcher

Published and distributed by: ESA Communication Production Office
ESTEC, Noordwijk, The Netherlands
Tel: +31 71 565-3408
Fax: +31 71 565 5433

Printed in: The Netherlands

Price: €20

ISBN: 978-92-9221-897-2

ISSN: 0379-4067

Copyright: © 2008 European Space Agency

Contents

| | | |
|-------|---|----|
| 1 | Introduction..... | 5 |
| 1.1 | Project Background and Objectives | 5 |
| 1.2 | State of the art..... | 6 |
| 1.2.1 | Commercially Available Chemical Conversion Coatings..... | 6 |
| 1.2.2 | Review of Published Papers | 9 |
| 2 | Experimental Phase | 17 |
| 2.1 | Materials, preparation of specimens, and treatments..... | 17 |
| 2.2 | Evaluation of the aluminium alloys samples..... | 17 |
| 2.2.1 | Surface roughness..... | 17 |
| 2.2.2 | Surface electrical resistivity..... | 18 |
| 2.2.3 | Thermal cycling tests..... | 18 |
| 2.2.4 | Salt spray tests | 18 |
| 2.2.5 | Scanning electron microscopy and energy dispersive X-ray spectrometry (SEM/EDS)..... | 19 |
| 2.2.6 | Chemical conversion coatings procedure | 19 |
| 3 | Results / Discussion..... | 21 |
| 3.1 | Visual inspection | 21 |
| 3.1.1 | 'As received' | 21 |
| 3.1.2 | 'As produced' | 21 |
| 3.1.3 | After thermal cycling tests..... | 21 |
| 3.1.4 | After salt spray tests | 21 |
| 3.1.5 | After thermal cycling + salt spray tests | 21 |
| 3.2 | Surface roughness..... | 29 |
| 3.3 | Surface electrical resistivity measurements..... | 30 |
| 3.4 | Surface morphology analysis - Scanning electron microscopy .. | 31 |
| 3.4.1 | After cleaning with Novaclean Al86 | 31 |
| 3.4.2 | After chemical conversion coating treatments..... | 32 |
| 3.4.3 | After thermal cycling tests..... | 39 |
| 3.4.4 | After salt spray tests | 43 |
| 3.4.5 | After thermal cycling plus salt spray tests..... | 47 |
| 3.4.6 | Comparison and correlation between Aluminium alloys and techniques performed | 51 |
| 4 | Conclusions..... | 57 |
| 5 | References..... | 59 |

Abstract

The most common conversion coating (CCC) currently used for improving the corrosion resistance of aluminium and its alloys that are used in the construction of ESA spacecraft is *Alodine 1200* manufactured by Henkel. This commercial product is a chromium (VI)-based chemical conversion coating. However, due to the environmental impact of hexavalent chromate, and recent EU regulations enforcing prohibition of the use of certain hazardous substances in electrical and electronic equipment, there is a great need for chrome (VI)-free anti-corrosion coatings.

The aim of this work was the study of commercially-available alternatives to chromium (VI)-based treatments. They should assure the same level of performance in terms of corrosion resistance, thermal and electrical properties. The objective of this study was to perform an assessment of commercially existing chemical conversion coatings for the protection of aluminium alloys that are to be used in the hardware of ESA space vehicles.

In this study, the aluminium alloys Al7075, Al2219 and Al5083 were used as substrates for evaluation of the chemical conversion coatings.

Among various chemical conversion coating systems, three alternative conversion coating pretreatments were selected for evaluation: Alodine 5700, Nabutan STI/310 and Iridite NCP. The chromium (VI) conversion coating Alodine 1200 was used as the reference.

The quality assessment of conversion coatings was evaluated by optical and scanning electron microscopy. Coated samples were characterised by salt spray exposure in order to simulate ground storage conditions; thermal cycling under vacuum, which simulates an in-orbit space environment; and electrical resistivity, as spacecraft sub-systems are electrically grounded to one another.

1 Introduction

1.1 Project Background and Objectives

Aluminium and its alloys are largely used on board space vehicles due to a good combination of specific weight and mechanical properties. Although space hardware for spacecraft use is usually confined to controlled environments, in emergency conditions, the pre-launching phase, or prolonged storage for reusable spacecraft, it may be exposed to harsh environments, such as the marine atmosphere that exists at coastal launch sites. This requires that all aluminium alloys must be protected by a proper anti-corrosion treatment. It is usual for all aluminium alloys to receive a pre-treatment and a coating scheme. The most successful pre-treatment for Al and Al alloys used so far are Chromium (VI) based chemical conversion coatings. A notable representative of this is a product commercially available under the brand name Alodine 1200.

Recent EU legislative restrictions enforced strong limitations to the use of chromate conversion coatings. Member states should ensure, from 1 July 2006, new electrical and electronic equipment put on the market shall not contain hexavalent chromium [1]. Exempted are materials and components in which design changes are technically, or scientifically, impracticable, or where the negative environmental, health and/or consumer safety impacts caused by the substitution are likely to outweigh the environmental, health and/or consumer safety benefits.

Although the aerospace and aeronautic industries have been exempted from compliance with the EU regulations, ESA is preparing itself to comply with the ROSH directive [1] and simultaneously to keep the lead in the search for an environmentally cleaner, socially responsible industry.

With this goal in mind, ESTEC contracted the Instituto de Soldadura e Qualidade, ISQ, to produce a benchmarking study on the viable alternatives for Cr (VI) based coatings. The main objective of this applied research work is to assess existing commercially-available chemical conversion coatings to be used as pre-treatments coating on aluminium alloys. Candidate pre-treatments for this study must:

- be industrially available for ready application;
- ensure at least the performance level achieved by current Cr (VI) pre-treatments
- include one coating having a European origin.

Further, technical performance requirements for viable alternative chemical conversion coatings in this study, are:

- good corrosion resistance to tropical environments: the European spacecraft launching base is located in the tropics, a region characterised by high humidity, high temperature and salty atmosphere;
- Good electrical properties: many Al alloys are used in the spacecraft as structural components. However, besides adequate mechanical properties, they must ensure proper electrical resistance in order to obtain an equipotential surface;
- Thermal properties: extreme temperatures can be achieved either in space ($\pm 100^{\circ}\text{C}$) or in prolonged storage condition, on Earth, often in tropical climates ($+50^{\circ}\text{C}$ and very high humidity).

In this study, Alodine 1200 (Henkel) will be used as the state-of-the-art chemical conversion coating.

Table 1 illustrates the aluminium alloys compositions used in this study.

Table 1 – Aluminium alloys, chemical composition [2].

| Aluminium alloy | Composition |
|-----------------|------------------------------------|
| Al7075 | 5.5% Zn; 2.5% Mg; 1.5% Cu; 0.3% Cr |
| Al2219 | 6.3% Cu; 0.3% Mn |
| Al5083 | 4.5% Mg; 0.7% Mn |

It should be noted that the low strength aluminium alloys (5000 and 6000 series) are permitted to have a final finish of chromate conversion coating. However, ESA prescribes in ECSS-Q-70-71 ('Data for the selection of space materials and processes'), that the high strength alloys (2000 and 7000 series) shall have a further painted finish applied to the chromate pre-treatment, or alternatively be anodised.

1.2 State of the art

In this section a literature survey of recently published studies related to chromate-free coatings has been performed.

1.2.1 Commercially Available Chemical Conversion Coatings

A study has been conducted in the USA under contract by the Deputy Undersecretary of Defense for Environmental Security. Its overall objective was to validate and implement multiple CHROMATE-free aluminium pre-treatment alternatives for a broad range of applications [4]. Alternatives studied were all aqueous solutions designed to obtain a thin coating on the substrate that would enhance paint adhesion and corrosion protection. Some of the alternatives provide unpainted corrosion protection as well as electrical conductivity in corrosive environments, especially in the 2xxx series alloys. The best results have been obtained with a Cr (III) based composition. The second best alternative, and the best of the chrome free alternatives, was Alodine 5200/5700, although it did not perform as well in unpainted applications as Navair Trivalent Chromium Pretreatment (TPC) did. Alodine 5200/5700 did not perform well against filiform corrosion, but was found to be process flexible and could be applied similarly to chromate conversion coatings.

NASA tested three alternative pre-treatments: Alodine 5700 (Henkel Corp.), Okemcoat 4500 (Oakite Products, Inc.) and Chemidize 727ND (MacDermid Inc.). Okemcoat 4500 was dropped from qualification due to poor performance during Bend Strength – Flexibility and Water Resistance qualification tests. The other two were found to be acceptable for flight. Alodine 5700 was classified as having flexible processing parameters and was recommended for implementation as a pre-treatment alternative. NASA changed to Alodine 5700, as part of their new Hentzen system (05510WEPX/05511CEH-X primer and 4636 WUX-3/4600CHA-SG topcoat) from Hentzen Coatings Inc. / Alodine 5700 in June 2002, and the first hardware flew in late 2002.

At the ASST 2006 Conference [5] a session was dedicated to Al pretreatments. This session started with an overview from Alcan R&D

concerning new alloys for aircraft application, namely Al-Cu-Li alloys. Some emphasis was also given to joining techniques with potential for application, namely laser beam and friction stir welding of panels. Furthermore, some studies with sol-gel coatings were presented [6-8]. Sepulveda *et al.* [5] implemented a sol-gel conversion coating process to produce a zirconium oxide coating on Al2024-T3 alloy, that was characterised morphologically and by electrochemical techniques. The coatings produced presented a uniform film, with no evidence of cracking or delamination. Polarisation studies revealed no breakdown potential up to +0.5 V (SCE), indicating an ennoblement of the pitting potential of over +1.0 V, at a low scan rate, and the passive region exhibited variations in the current density that suggest a self-healing capacity of the coating. This study allowed establishing conditions for optimisation of zirconia sol-gel coatings for structural aluminium alloy, using electrochemical impedance spectroscopy. Hughes *et al.* [7] studied the performance of a cerium tridibutylphosphate-based inhibitor for corrosion of aluminium alloys. Raman spectroscopy and SEM/EDS were used to characterise the reactions of Al2024-T3 with Ce(dbp)₃ solutions in the presence of NaCl.

Raps *et al.* [8] tested alternative systems based on permanganate, cerates, zirconate and trivalent chromium, which form a chemically-growing oxide film in a traditional tank process. Also investigated was a different approach based on organic-inorganic hybrid sol-gel coatings and silane films, which can develop an oxide layer on the natural aluminium oxide by formation of covalent Al-O-Si bonds. Thus, those coatings offer the possibility to link the metal oxide and the organic coating (primer). The film morphology and corrosion protection properties were studied by SEM, salt spray test, filiform corrosion test and electrochemical test methods. They concluded that the trivalent chromium-based conversion coating and the sol-gel coatings are able to close the gap between barrier functionality and adhesion promotion. The chromium (III) process was reported to have the most promising performance of all the chemical conversion coatings tested, being the best alternative and thus the most effective substitute for Cr (VI) based conversion systems.

Under this present ISQ-ESA research contract, contacts with different suppliers (HENKEL, ATOTECH, CHEMO-PHOS, SURTEC, MacDermid, Kluthe and Enthone, Alcan) were undertaken for an update on alternative industrial chemical conversion pretreatments. However, only some of these companies sent pre-treatment solution samples and product information, namely Henkel (by Henkel Ibérica Surface Technologies), CHEMO-PHOS, SURTEC and MacDermid (through its sales representative in Portugal, Artergalva Lda.).

An overview of the alternative chemical conversion pretreatments, as well of the conventional chromium based coatings is described.

a) Alodine 1200S (Reference) [9]

Alodine 1200S (Henkel Surface Technologies) is a hexavalent chromium based chemical conversion coating. In this study it will be the reference for this pretreatment evaluation. Alodine 1200S treated surfaces have an excellent corrosion resistance, and an increase in the paint adherence. The immersion bath has a long term stability and does not often need to be replenished. The solution can be used by immersion, spray or wipe processes. The immersion bath has a long term stability and does not often need to be replenished. The pretreatment by immersion is performed at

temperatures in the range of 25-35°C for 15 seconds to 3 minutes, adjusting the pH 1.3 to 1.8.

Furthermore, ALODINE 1200S treated surfaces have colours ranging from a light iridescent golden to tan, depending on alloy and coating thickness.

b) Henkel Alodine 5200/5700 [4, 10]

Alodine 5700 (Henkel Surface Technologies) is a chromium-free conversion coating, formulated as a ready-to-use material for spray or immersion application, and is a diluted form of the Alodine 5200. The solution is used in a similar fashion to conventional chromate pretreatments and is performed at a temperature of 25-35°C for 1-5 minutes. Alodine 5200/5700 is an organometallic zirconate complex based pretreatment. Deposited coatings have a light colour ranging from blue to tan, depending on the alloy [4].

c) Sanchem Safeguard 7000 with seal [4]

It is based on potassium permanganate, with a complex sealant composed of polyacrylic acid polypropylene glycol and fatty acid esters. It is processed as a two-component product (one solution potassium permanganate, and one seal). The pretreatment is performed at room temperature; however, it requires high temperatures for seal cure (about 92°C, 200°F). Application is performed by immersion, spray, and wiping. It induces a bronze gold colour coating.

d) Surtec Chromital TPC [11]

On a benchmarking performed by Surtec, using Alodine 1200S as reference, Surtec 650 pretreatment presented very similar performance characteristics to the control product. Surface preparation is dependent on the silicon content of the alloy: for Al alloys containing less than 1% Si, surface preparation includes alkaline degreasing, alkaline etching and deoxidation; for Al alloys containing more than 1% Si, surface preparation does not require the alkaline etching step.

In application by immersion, Surtec 650 is to be applied in a 20% concentration in deionised water. The solution pH must be adjusted to 3.9 (3.7 – 3.95), with sulphuric acid or sodium hydroxide. The pretreatment is to be performed in the range 30-40°C. This temperature will influence the bathing time. Pre-treatment times range from 0.5 to 4 minutes.

e) Nabutan STI/310 [12]

Nabutan STI/310 is a chrome-free, no-rinse, mixture of inorganic and organic acids composed fundamentally of fluorotitanic acid and can be applied to the surface treatment of aluminum alloys. The corrosion resistance and the adherence of subsequent paint coats to the treated surface will be improved. This coating is applied preferentially by dipping and spraying.

f) Iridite NCP [13]

The Iridite NCP is a chromium-free passivation treatment designed specifically for aluminium and its alloys; it provides both high adhesion values for paints and powder coatings, and excellent corrosion resistance. Iridite NCP also has the ability to withstand high temperatures, so it is suitable for use on items that require high operating temperatures. This unique property, not found on chromates, also allows applicators to increase

the temperature of their dry-off ovens prior to painting. Unlike traditional chromate treatments that require 24 h to cure to a hard film, Iridite provides a hard amorphous crystalline coating as formed. The IRIDITE NCP coating is normally clear at low coating weights to a light blue colour at highest coating weights. There are times when the coating is iridescent due to refraction of light by the conversion coating. The colour is very much dependent on the chemical processing conditions, substrate alloy and surface condition being processed. Because of this, coating quality cannot be assessed by judging the colour of the coating [14].

Based on the properties of each of the commercially-available chemical conversion coatings mentioned above, ESA and ISQ selected three of them for evaluation.

The chromium (VI) conversion coating Alodine 1200 will be used as reference. The characteristics of these chemical conversion coatings are summarised in Table 2 [9, 10, 12 and 13].

Table 2 – Summary of chromate and chromium-free conversion coatings.

| Conversion coating | Chemistry (from MSDSs) | Application Methods | Advantages | Disadvantages |
|--|----------------------------------|------------------------|--|--|
| Alodine 1200S <i>Reference</i> (Henkel, Germany) | Chromic acid, complex fluorides | Immersion, spray, wipe | Easy to use; standard | Contains hexavalent chromium |
| Alodine 5700 (Henkel, Germany) | Organometallic zirconate complex | Immersion, spray, wipe | Easy to use; drop-in replacement for chromates | Minimal corrosion inhibition; unperceivable colour change |
| Nabutan STI/310 (Chemo-Phos, Germany) | Fluorotitanic acid | Immersion, spray | Easy to use; chromium-free | Minimal corrosion inhibition; Colourless |
| Iridite NCP (MacDermid, USA) | Probably fluorotitanate based | Immersion, spray | Easy to use; chromium-free | Minimal corrosion inhibition; Colour depends on the chemical processing conditions and alloy |

1.2.2 Review of Published Papers

Chromate conversion coatings (CCC) have been intensively studied over the past decades due to the effective corrosion protection they confer on Al alloys and the desire to develop an effective and environment-friendly replacement. The composition and structure of CCCs formed on pure Al and Al alloys have been investigated using a variety of analytical tools [15].

The influence of surface preparation on performance of chromate conversion coatings on Alclad 2024 aluminium alloy was investigated by Campestrini *et al.* [16, 17]. Since the parameters of each pretreatment step, performed before the chromating process, give rise to important modifications of the morphology and microstructure of the aluminium surface, they strongly influence the nucleation and growth of the chromate layers, and therefore, their final properties. Researchers studied the influence of both the immersion in a nitric-hydrofluoric acid solution, carried out between the acid pickling step (immersion in sulfuric-phosphoric acid solution) and the chromating step, and the duration of the acid pickling step on the surface

properties of Alclad 2024-T3 aluminium alloy was studied. Scanning Electron Microscopy (SEM), Atomic Force Microscopy (AFM) and electrochemical investigations highlighted the fact that this intermediate step in the pretreatment route gave rise to a more etched but less reactive surface, due to the removal of a large number of cathodic sites, mainly related to Al-Fe-Si phases present in the clad layer. A similar effect, but on a smaller scale, was caused also by the increase of immersion time in sulphuric-phosphoric acid solution. The decrease of galvanic coupling gives rise to a more homogeneous nucleation of the chromate conversion coating on the surface of the Alclad 2024-T3. Moreover, the chromate film tends to be denser and with fewer defects. In fact, removal of galvanic coupling from the aluminium surface appears to be a requirement for the formation of a chromate layer with good corrosion resistance [17]. Besides, the surface properties of the aluminium substrate largely influence the morphology and composition, not only of the chromate film but also of the corrosion products formed at weak spots, which seem to play an important role in the level of protection provided by the chromate conversion coating.

Waldrop and Kendig [18] studied the formation of CCC on AA2024-T3 using AFM. The CCC on the Al matrix was found to nucleate and grow very fast in the form of nodules. Nucleation and growth of the coating were faster on Al-Fe-Cu-Mn particles than on Al-Cu-Mg. A similar AFM study of nucleation and growth of CCC formed on AA2024-T3 in combination with FE-SEM and TEM, was conducted by Brown and Kobayashi [19]. They concluded that CCC formation and growth on intermetallics strongly depended on the size, shape and composition of intermetallics.

Sun *et al.* [20] used SEM, transmission electron microscopy (TEM), and X-ray photoelectron Spectroscopy (XPS) to examine chromate coatings formed on 2024-T3 samples, to which different pre-treatments had been given. These samples have also been evaluated for their corrosion behaviour. Although a previous work has shown that different pre-treatments can directly influence the compositions at surface regions of Al alloys, this work highlights the fact that this initial enrichment can affect the composition and properties of a subsequent conversion coating. The present study for chromate coating provides a good reference for comparison with parallel work being done on alternative non-chromated coatings.

Treacy *et al.* [21] carried out several surface analysis studies on chromate conversion coated 2014-T6 aluminium alloy prior to, and after exposure to a neutral sodium chloride salt fog environment. The development of dark stains on surfaces after 48 h of salt spray fog exposure coincided with the loss of chromium, indicative of the coating failure. This fact was observed by surface analytical techniques: XPS, AES (Auger electron spectroscopy) and LIMA (Laser induced mass analysis). From LIMA analysis it would appear that these regions are associated with copper-containing intermetallics, suggesting that chromate coating deterioration during salt fog exposure occurs at highly active copper-containing intermetallic sites.

Lunder *et al.* [22] investigated the role of microstructure in the formation of a chromate conversion coating on extruded AA6060. The surfaces were given a conventional surface treatment, involving alkaline etching and deoxidation prior to treatment in a commercial chromate solution (Alodine C6100). The coated surfaces were examined by surface analytical techniques and electrochemical techniques. A non-uniform growth of the chromate conversion coating (CCC) on AA6060-T6 resulted in a porous morphology, with cracks extending down to the base metal. Poor coverage was particularly observed at the grain boundaries.

It is generally accepted that CCCs form via a redox reaction between Al in the alloy and Cr (VI) species in the chromating solution. They are amorphous and mainly composed of hydrated mixed Cr (III) /Cr (VI) oxide. The Cr (VI) species can be stored in CCC and released as soluble chromate species when CCC is exposed to solution. This characteristic of CCC is believed to lead to the important 'self-healing' ability of CCC-treated alloys. Chromate conversion coatings (Alodine 1200S) on AA7075-T6 were characterised by Meng *et al.* [23] using SEM, focused ion beam sectioning and s-TEM with nanoelectron dispersive spectroscopy line profiling. The CCC formed on AA7075 is heterogeneous and the coating formed on the Al matrix was much thicker than that formed on the coarse Al–Cu–Mg, Al–Fe–Cu and Mg–Si intermetallic particles. The coating formation on the intermetallics has been shown to be dependent on the electrochemical reactivity of the intermetallics, the local pH change and the interaction of the intermetallics with HF and ferricyanide.

A review by Kending *et al.* [15] of studies carried out on aluminium and aluminium alloys, showed that the oxoanions of hexavalent chromium uniquely inhibit the corrosion of many metals and alloys. They are particularly useful for protecting the high strength aluminium alloys against corrosion. The inhibition of Al corrosion is derived from both inhibition of oxygen reduction and inhibition of metal dissolution reactions, mainly due to a delay in the onset of pitting. Inhibition of corrosion by chromates appears to be closely linked to their ability to irreversibly adsorb on to metal and oxide surfaces.

In order to characterise filiform corrosion on a commercial AA2024-T351 aluminium alloy, a detailed microscopic study using SEM and EDX was performed by Mol *et al.* [24]. Some of the aluminium alloy samples were alkaline-cleaned, deoxidised, and coated with a chromate conversion and others were only alkaline-cleaned before coating. Both samples were similarly spray-coated with a 42 µm clear polyurethane topcoat. Cross section and top views examined by SEM revealed varying degrees of attack ranging from generalised etching without local attack, to severe local attack in the form of pitting, resulting in grain etchout, grain boundary attack and subsurface etchout. EDS revealed the presence of chloride inside the pits, and subsurface etchout.

Characterisation of the metal-coating interface is crucial to the understanding, and prediction of the corrosion protective-coatings performance. Bierwagen *et al.* [25] reported the use of different methods to examine the interface between steel and marine coatings and to image the surface of a) untreated and b) chromate/phosphate treated aircraft aluminium alloys. Electrochemical noise (EN), EIS and Prohesion™ testing were performed in parallel with AFM/SEM measurements. They proved to be beneficial in the characterisation of surface morphology, corrosion resistance properties of coatings and possibly for determining mechanisms of corrosion. The e-coat systems displayed resistance values higher than the spray coat systems and their delamination areas were lower, indicating they are better for corrosion control for undamaged systems.

Fedrizzi *et al.* [26] studied the effect of chemical cleaning (alkaline, acid, combination of the two) and environmentally-friendly and chromate pre-treatment baths on the filiform corrosion behaviour of aluminium AA6060 alloys. They concluded that the poor behaviour of samples cleaned in an alkaline bath can be related to a remarkable chemical surface modification induced by the chemical etching. In fact, after this alkaline etching, the aluminium surface was found to be highly enriched in elements like copper, zinc or magnesium, which has been shown to affect the filiform corrosion

resistance to varying extents. The use of acid cleaning after the alkaline etching allowed a significant improvement of the aluminium surface chemistry, and consequently the filiform corrosion resistance. The best behaviour was obtained by chromate or fluorotitanate conversion coatings after an alkaline plus acid chemical cleaning.

Zhao *et al.* [27] studied the effects of chromate conversion coatings (CCC) and chromate in solution on the corrosion behaviour of AA2024-T3, and pure Al. The influence of the chromate on pit growth was studied by the thin film pit-growth technique. The release and migration of chromate from CCCs and the comparison of the CCCs chemistry with various synthetic mixed oxides composed of Al (III), Cr (III) and Cr (VI) species, was investigated by Raman spectroscopy. The effect of released chromate was also studied by electrochemical methods. Using an artificial scratch cell, chromate released from CCCs was seen to migrate to, and protect, a nearby uncoated area. However, experiments investigating the effect of chromate in solution on the anodic dissolution kinetics under potentiostatic control indicated that large chromate concentrations were needed in order that an effect can be seen.

John Bibber [28] published an overview of non-hexavalent chromium conversion coatings that could provide excellent corrosion resistance and paint adhesion characteristics when used with aluminium and its alloys, compared with the chromium-based conversion treatment. The four main types of conversion coatings in common use are based upon:

- 1) The formation of a chromium hydroxide and/or chromium oxide film;
- 2) The production of a precipitated heavy metal phosphate or oxide film;
- 3) The use of various synthetic polymers, with or without heavy metal phosphates or oxides; and
- 4) The formation of a manganese oxide/aluminium oxide film by use of permanganates.

The author concluded that the manganese oxides produced by the heptavalent-manganese-based system are by far the most closely related to the chromium oxides and hydroxides in terms of their respective chemistries. Thus, the aluminium oxide/manganese oxide film, as produced by the heptavalent-manganese conversion coating system, is the alternative pre-treatment most closely matching the actual CCC in terms of actual chemistry and performance.

NCAP ('Non-Chromate Aluminum Pretreatment Project') [4] has undertaken a project to validate, and implement, multiple chromate-free aluminium pretreatment alternatives. The researchers concluded that all alternatives tested showed acceptable performance. From the evaluated chemical coatings, the only pretreatments that came close to matching the technical performance, cost and flexibility of chromates are those based on trivalent chromium (Navair TCP). Furthermore, the Alodine 5200/5700 pretreatment performed similarly to TCP in most painted systems, but not in unpainted applications. In general, although none of the other selected pre-treatments can compete with the overall performance of these two pretreatments, many could be selected for specific coating system applications, and achieve the desired performance.

Cerium-based Al and Al-alloy pre-treatments have been proven as efficient, environmentally-clean alternatives to the environmentally-undesirable Cr (VI) compounds. Thus, full immersion in cerium salt solutions allows an identical corrosion protection level to that of chromate-based treatments. A

major drawback is that treatment time is too long for industrial applications [29].

Bethencourt *et al.* [30] proposed accelerated methods for obtaining cerium-rich conversion coatings on aluminium-magnesium alloys (Al5083). The films developed have been characterised by SEM and EDS. These studies revealed that the coatings have a mixed or heterogeneous nature, being composed of a layer of alumina covering the matrix, together with islands of cerium formed over the cathodic intermetallics present on the alloy surface. Furthermore, electrochemical studies indicate that the protection level provided by these coatings is several orders of magnitude higher than achieved with other treatments, such as chromate-based treatment.

Work by Arnott *et al.* [31] has shown that cerium-based coating deposition relies on electrochemical interactions between the aluminium matrix and intermetallic inclusions that make up structural aluminium alloys.

Fahrenholtz *et al.* [32] studied the performance of a cerium-based conversion coating formed by spontaneous reaction between a water-based solution containing CeCl_3 and aluminium alloy 7075-T6 substrates. This study has shown that the cerium conversion coating morphology and salt fog performance were affected by the type of pre-treatment of the panel prior to coating. The best pre-treatment consisted of desmutting, degreasing, and acid activation.

Rivera *et al.* [33] developed an improved process for the spontaneous deposition of cerium oxide conversion coatings for corrosion protection of aluminium alloy 7075-T6, by a spontaneous dip-immersion process that resulted in improved salt fog corrosion performance. The role of substrate surface preparation and post-treatment was discussed in terms of the surface morphology, thickness and performance of coatings on aluminium alloy 7075-T6.

Decroly *et al.* [34] investigated a chromate conversion coating alternative treatment (cerium salt-based conversion) that could meet all the requirements for industrial application. The corrosion protection properties of this Ce conversion coating were investigated by cathodic and anodic polarisation measurements and by electrochemical impedance spectroscopy (EIS). However, although the coatings formed presented interesting properties, their performances did not match those of chromate conversion coatings.

The cerium-based chemical conversion coating is an effective method to improve the resistance to localised corrosion of the aluminium borate whisker reinforced AA6061 composite ($\text{Al}_{18}\text{B}_4\text{O}_{33}\text{w}/6061\text{Al}$). Hu *et al.* [35, 36] reported a cerium conversion coating formed by an immersion process that resulted in improved salt spray corrosion performance. The CeCl_3 concentration in the test solution has been shown to have a significant influence on the corrosion behaviour, and surface morphologies of the coated samples.

The electrochemical behaviour of a Ce conversion coating formed on Al alloy 2024-T3 covered with a Cu-rich smut has been studied by Palomino *et al.* [37]. The microstructural characterisation has shown that the precipitation of the Ce conversion layer seems to occur homogeneously in the presence of the Cu-rich smut originating a uniform coating. Moreover, it has been confirmed that the dry-mud structure of this kind of conversion layer is just a superficial phenomenon, with only a few cracks attaining the metallic substrate, most likely due to stress relieving. Electrochemical results and SEM/EDS characterisation have evidenced the self-healing properties of the

Ce conversion layers, which allow ions released from the coating to precipitate above active sites during the immersion of the coated metal in an aggressive electrolyte.

The same researchers investigated the corrosion behaviour of a bi-layer cerium-silane pretreatment on Al 2024-T3 in 0.1 M NaCl [38], by electrochemical techniques (anodic polarisation curves and electrochemical impedance spectroscopy (EIS)). EIS has shown a continuous increase of the impedance response during the whole test period, which was interpreted on the basis of a pore-blocking mechanism. This theory was supported by SEM observation and equivalent circuit fitting. On the other hand, mechanical tests have evidenced the good adhesion of the silane layer to the Ce conversion layer, which has been interpreted as a better linking between the silane molecules and the cerium bottom layer.

Hughes *et al.* [39] studied filiform attack on a cerated AA2024-T351 aluminium alloy with a polyurethane topcoat by SEM/EDS. The observations revealed that filiform corrosion results were similar to those obtained on chromated and coated surfaces. This conclusion led to development of a filiform corrosion model, attributing the main cause of delamination to the volume expansion of the corrosion product.

Guan *et al.* [40] published an overview describing the formation, chemistry, morphology, and corrosion protection of a new type of inorganic conversion coating. This coating, referred to as a vanadate conversion coating (VCC), forms on aluminium alloy substrates in a matter of minutes by deeping the substrate in aqueous vanadate-based solutions at ambient temperatures. Electrochemical testing was used to confirm earlier reports of Al corrosion inhibition by soluble vanadates, which showed that in near-neutral solutions, vanadate increases the pitting potential, and decreases the oxygen reduction reaction rate on AA2024-T3. Impedance experiments suggest that slow film formation may be occurring on Al in contact with vanadate-bearing solutions.

Khoabaib *et al.* [41] evaluated the corrosion resistance behaviour of a proprietary sol-gel based coating system, as replacement for Alodine 1200, on Al2024 alloys. The sol-gel method is also being applied to obtain a thin protective coating of cerate, molybdate and other rare-earth compounds on the aluminium substrate through environmentally-friendly processes. The performance of this coating evaluated by electrochemical techniques concluded that the sol-gel treated E-coat provided an acceptable corrosion protection level, similar to that of the conventional chromate system.

Yang *et al.* [42] investigated the behaviour of a SiO₂ and ZrO₂ sol-gel conversion coating, both alone and in combination with a polyurethane uniconat (TT-P-2756, self-priming topcoat) on Al 2024-T3 alloy. The evolution of the coating system under immersion was followed by AFM, SEM, EIS, and XPS. Although after two days of immersion, pitting corrosion and degradation products on the sol-gel single coating surface were observed, further pitting corrosion ceased after a few days of immersion. Undercoating blisters in the sol-gel plus polyurethane topcoat system were found at 4 weeks of immersion, after which no further increase in blister size was observed. Results are explained based on a theory that after initial corrosion, aluminium and silicon oxides may form a stable mixed-oxide barrier layer at the interface hindering further pitting corrosion.

Parkhill *et al.* [43] demonstrated that an epoxide modified silicate sol-gel film spray coated on aluminium alloy 2024-T3 panels provides exceptional barrier and corrosion protection when compared to chromate-based surface treatments (Alodine 1200). The ormosil film was characterised using

profilometry, optical spectroscopy, and electrochemical analysis. The authors concluded that a spray-coated water-based environmentally-compliant sol-gel coating exhibits great potential for the replacement of the chromate-based conversion coatings presently used in the corrosion-prevention scheme of aircraft aluminium.

CCC on Magnesium Alloys

Zhao *et al.* [44] reported on the chromium-free conversion coating performance for application on magnesium alloys. In one of these works the researchers studied the coating performance of phosphate-permanganate treatment that adopted phosphate, incorporated with di-potassium hydrogen phosphate and permanganate, on magnesium alloys. They concluded that this treatment is capable of producing uniform coatings and with reasonable adhesion to the substrate. Furthermore, the results of the corrosion testing showed that the coating corrosion resistance was equivalent to the protection afforded by the traditional chromate treatment.

The same authors [45] developed a chromium-free multi-element complex coating (MEEC), that was obtained using a new kind of chemical conversion process and an environmentally-friendly treatment technique. The composition and microstructure of the coating layer formed on magnesium alloys were characterised and showed good corrosion resistance.

The growth process of the same multi-element complex coating (MECC) on magnesium alloy was also studied [46]. The morphological and structural composition of the coatings studied by SEM, EDX, XRD and AFM, allowed the conclusion that coating formation is a three-stage process: initial stage with formation of a compact, amorphous layer; metaphase stage where the intermediate layer consists of a mixture of amorphous and crystalline material, and a final stage, in which the crystallinity increases and the coating surface becomes smooth and compact.

The degradation process of a chromium-free conversion coating on Mg alloys was investigated in NaCl solutions [47], by EIS, and a mathematical model for the degradation mechanism was proposed.

The development of a potassium permanganate bath chemical conversion coating for magnesium alloys was investigated by Umehara *et al.* [48]. The coating formed consisted of an amorphous film composed mainly of manganese oxides, magnesium oxide or hydroxide.

The corrosion protection supplied by an aluminium arc-spray coating, post-treated by hot pressing and anodising on an AZ31 magnesium alloy, has been studied by Chiu *et al.* [49] by using electrochemical polarisation and EIS. In this study, the Al arc-spray coating as well as a post-hot pressing and anodising treatment were carried out on an AZ31 Mg alloy, and the effect of the processing on the corrosion resistance was evaluated. The corrosion in the Al-sprayed AZ31 specimen was enhanced by a galvanic cell occurring at the interface of the Al coating and the AZ31 substrate, under the circumstances when electrolyte was supplied through the porous Al coating to the interface region.

Montemor *et al.* [50] investigated the composition and corrosion resistance of cerium conversion films on the AZ31 magnesium alloy and its relation to the salt anion. For that purpose, pretreatments based on different cerium (III) salts were performed by immersion of Mg alloy in a solution of cerium chloride, cerium nitrate, cerium sulphate and cerium phosphate. The chemical composition of the treated surfaces was investigated by X-ray photoelectron spectroscopy and Auger electron spectroscopy, whereas the corrosion behaviour of the pretreated AZ31 substrates was investigated in

0.005 M NaCl solutions, using potentiodynamic polarisation and open-circuit potential monitoring. The results showed that the chemical composition and the corrosion protection ability are dependent on the cerium salt used for the deposition of the conversion layers. Conversion layers obtained by immersion in CeCl_3 are the thickest and the most protective. The electrochemical results show that all the conversion pre-treatments reduced the corrosion activity of the AZ31 Mg alloy substrates in the presence of chloride ions. The corrosion protection efficiency is related to the anion present in the cerium salt.

In previous work performed by the same authors [50] it was demonstrated that conversion pre-treatments based on cerium nitrate or lanthanum nitrate could protect the AZ31 Mg alloy, the effectiveness of the conversion layer being dependent on the treatment time. Electrochemical and analytical techniques were combined to study the rare-earth conversion films formed on the AZ31 Mg alloys and their ability to provide corrosion protection. Cerium and lanthanum conversion layers provide corrosion protection on the AZ31 Mg alloy. The corrosion protection seems to be independent of the chemical composition of the conversion layer, however it does depend on the thickness.

Magnesium-rich coatings present a new and challenging field of development for the corrosion protection of aluminium structures [52]. These coatings are capable of sacrificial protection, but assessment of their efficiency and durability can be strongly affected by the testing environment. The corrosion behaviour of two aluminium alloys (Al2024 and Al7075) coated with a magnesium-rich coating, also of pure magnesium and of the bare aluminium substrates, was assessed in the two solutions (0.1% NaCl and dilute Harrison solution, DHS) using electrochemical techniques (OCP and EIS). The corrosion rate of pure magnesium was higher in DHS, although the dissolution rate of the magnesium embedded in the polymer matrix was not significantly affected. The impedance spectra of the scribed samples resembled that of the bare substrates in NaCl solution but not in DHS.

2 Experimental Phase

2.1 Materials, preparation of specimens, and treatments

Specimens of three aluminium alloys (Table 3) were mechanically cut in 4 x 4 cm dimensions and used as received for coating with the chemical conversion coating treatments selected for evaluation. For each pair, chemical conversion coating / aluminium alloy triplicates were prepared.

Table 3 – Chemical composition of aluminium alloys selected (wt %).

| Alloys | Al | Cu | Mg | Mn | Fe | Zn | Cr | Si | Ti |
|--------|------|---------|---------|---------|-------|---------|-----------|-------|----------|
| Al7075 | Bal. | 1.2-2.0 | 2.1-2.9 | 0-0.3 | 0-0.5 | 5.1-6.1 | 0.2-0.4 | 0-0.4 | 0-0.2 |
| Al2219 | Bal. | 5.8-6.8 | 0-0.02 | 0.2-0.4 | 0-0.3 | 0-0.1 | - | 0-0.2 | 0.02-0.1 |
| Al5083 | Bal. | 0-0.1 | 4.0-4.9 | 0.4-1.0 | 0-0.4 | 0-0.25 | 0.05-0.25 | 0-0.4 | 0-0.15 |

To assure that the metal surface was free from oil, grease and other foreign matter before the treatment, an appropriate cleaner was used. Because of its availability, Novaclean Al86 was used. This is a cold degreaser for aluminium used in immersion processes, combining degreasing and deoxidising characteristics.

2.2 Evaluation of the aluminium alloys samples

The following tests were performed on the samples.

Table 4 – Tests performed on aluminium alloys samples.

| | 'As received' | 'Cleaned' | 'As produced' (coated) | After thermal cycling | After SS exposure |
|------------------------------------|---------------|-----------|------------------------|-----------------------|-------------------|
| Surface roughness | X | X | X | X | - |
| Surface electrical resistivity | - | - | X | X | - |
| Thermal cycling* | - | - | X | | - |
| Salt spray (ASTM B117/07) | X | - | X | X | - |
| Scanning electron microscopy (SEM) | X | X | X | X | X |

* The thermal profile corresponds to a standardised profile of -50°C and +100°C, with dwell times of 15 min, at cooling/heating rates of 10°C/min;

2.2.1 Surface roughness

The surface roughness of the test panels was measured using a Mitutoyo SurfTest 201. A stylus attached to the detector unit of the SJ-201P is displaced at constant speed across the sample's surface, tracing surface irregularities. The vertical stylus displacement produced during tracing of the sample's surface is converted into electrical signals. The parameter used for expressing roughness was R_a , which is the arithmetic mean of the absolute values of the profile deviation from the centre line within the evaluation length [53].

2.2.2 Surface electrical resistivity

Surface resistivity could be defined as the material's inherent surface resistance to current flow multiplied by the ratio of the specimen's surface dimensions (width of electrodes divided by the distance between electrodes), which transforms the measured resistance to that obtained if the electrodes had formed the opposite sides of a square [54]. Surface resistivity does not depend on the physical dimensions of the material.

The surface electrical resistivity of the test panels was carried out with a Microohmmeter Schuetz Messtechnik, model MR 300C, based on the 4 point method. The resistance measured is then calculated through the equipment by applying Ohm's Law. The measured electrical resistance is proportional to the length of the sample and to the surface resistivity, and inversely proportional to the cross-sectional area of the sample:

$$\rho = (R \times S) / l$$

where:

ρ = surface electrical resistivity (Ω m);

R = electrical resistance of a uniform specimen of the material (Ω);

S = cross-sectional area of the specimen (m^2);

l = length of the specimen (m).

2.2.3 Thermal cycling tests

Thermal cycling is a test consisting of cycling a sample between two extreme temperatures which are held for a certain amount of time. The temperature change is performed at a constant rate. This is done for a specified number of cycles. As samples heat up and cool down they expand and contract, possibly causing fatigue or adhesion failure of the coating over time [55].

The thermal cycling tests were performed in air using a thermal chamber ARALAB, model Fitoterm 300. The thermal profile corresponds to a standardised profile of -50°C and $+100^{\circ}\text{C}$, with dwell times of 15 min., at cooling/heating rates of $10^{\circ}\text{C}/\text{min}$. The 500 cycles test was interrupted at the 200th cycle, for resistivity measurements.

2.2.4 Salt spray tests

Neutral salt spray testing was carried out according to ASTM B117 [56] with a 5% NaCl solution, at 35°C . The panels were placed in the cabinet between $15 - 30^{\circ}$ from the vertical, for 7 days. Photographic recording was performed each 24 h. The test panels were not allowed to contact other surfaces in the chamber and condensed or corrosion products on their surfaces were not permitted to cross-contaminate each other. After exposure, test panels were rinsed in deionised water to remove salt deposits from their surface and then immediately dried.

The salt spray exposure was carried out in a salt spray chamber ERICHSEN, model 606/400 L.

The samples were subsequently stored in a desiccator.

2.2.5 Scanning electron microscopy and energy dispersive X-ray spectrometry (SEM/EDS)

Surface morphology and chemical composition of the samples was performed on a scanning electron microscope JEOL-JSM model 6700, equipped with an Oxford energy-dispersive X-ray spectrometer (EDS), operated at 20 keV.

2.2.6 Chemical conversion coatings procedure

Figure 1 summarises treatment steps to which samples were submitted. The chemical conversion coatings were treated according to the respective technical data supplied (see Annexes).

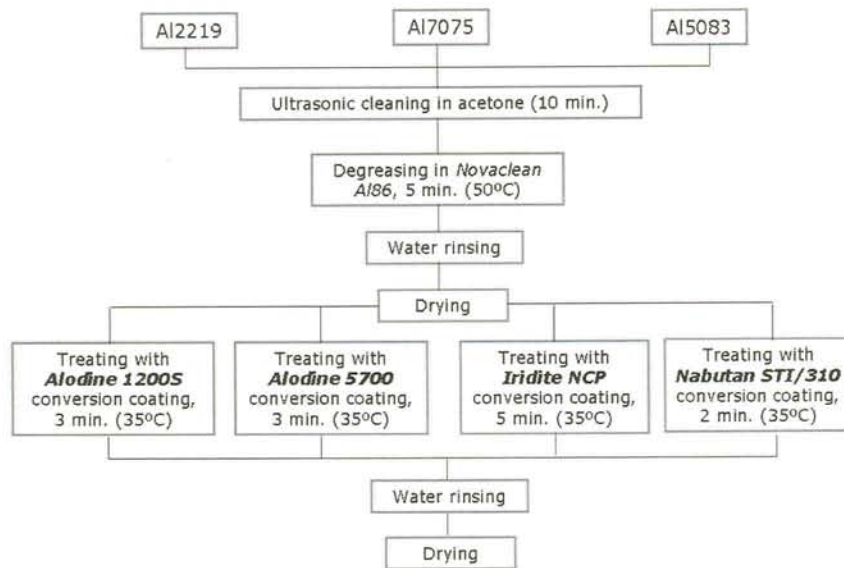


Figure 1 - Cleaning and treatment processes scheme.

3 Results / Discussion

3.1 Visual inspection

3.1.1 'As received'

The Al2219 test specimen 'As received' presented a visually rougher surface compared to the Al7075 and Al5083 aluminium alloys, as shown in Figure 2.

3.1.2 'As produced'

Figure 3 shows the test panels surfaces after application of the chemical conversion coatings:

- Alodine 1200S tested specimen surface presented an iridescent golden colour for all the alloys;
- Alodine 5700 provided a light golden appearance brighter on Al 2219;
- Iridite NCP gave colours ranging from light blue (Al 2219 and Al 7075) to yellowish (Al 5083) over the samples' surfaces;
- Nabutan coated samples kept the initial metallic aspect, and appeared colourless.

All pre-treatment coatings applied on Al2219 kept a mirror-like aspect of the surface. This can perhaps be interpreted as the deposited films in this alloy not being as thick as the other substrates.

3.1.3 After thermal cycling tests

The thermal cycling test did not produce visible changes in the samples (Figure 4). No cracks, delamination, or other form of degradation after thermal cycling exposure were observed.

The only visible effect of thermal cycling on the treated test panels was to darken the coating colours, probably as a result of dehydration caused by the combined effects of thermal contraction and expansion due to the temperature changes applied during the tests.

3.1.4 After salt spray tests

Figure 6 illustrates the coated test panel surfaces after the exposure to salt spray test:

- There is no evidence of corrosion on the three types of aluminium test panel coated with the Alodine 1200S, after 7 days of exposure;
- Alodine 5700 and Nabutan coatings showed surface corrosion within 24 h on Al7075 and Al2219, with formation of pits;
- Iridite NCP presents some corrosion on Al7075 and Al2219 after 48 h of exposure;
- There is no evidence of corrosion on the Al5083 coated samples after 7 days of exposure, for each of the treatments studied.

3.1.5 After thermal cycling + salt spray tests

Figure 7 shows the coated test panel surfaces subjected to thermal cycling measurements after the exposure to salt spray test. The results are very similar to those obtained for the samples after salt spray test:

-
- There is no evidence of corrosion on Al7075 and Al5083 test panels coated with the Alodine 1200S, after 7 days of exposure;
 - Al2219 samples coated with Alodine 1200S present some evidence of corrosion after 7 days of exposure;
 - Alodine 5700 and Nabutan coatings presented surface corrosion on Al7075 and Al2219 alloys, within 24 h of exposure; formation of pits;
 - Iridite NCP shows some corrosion on Al7075 and Al2219 after 48 h of exposure with formation of pits;
 - There is no evidence of corrosion on the Al5083 coated samples after 7 days of exposure, for each of the treatments studied.

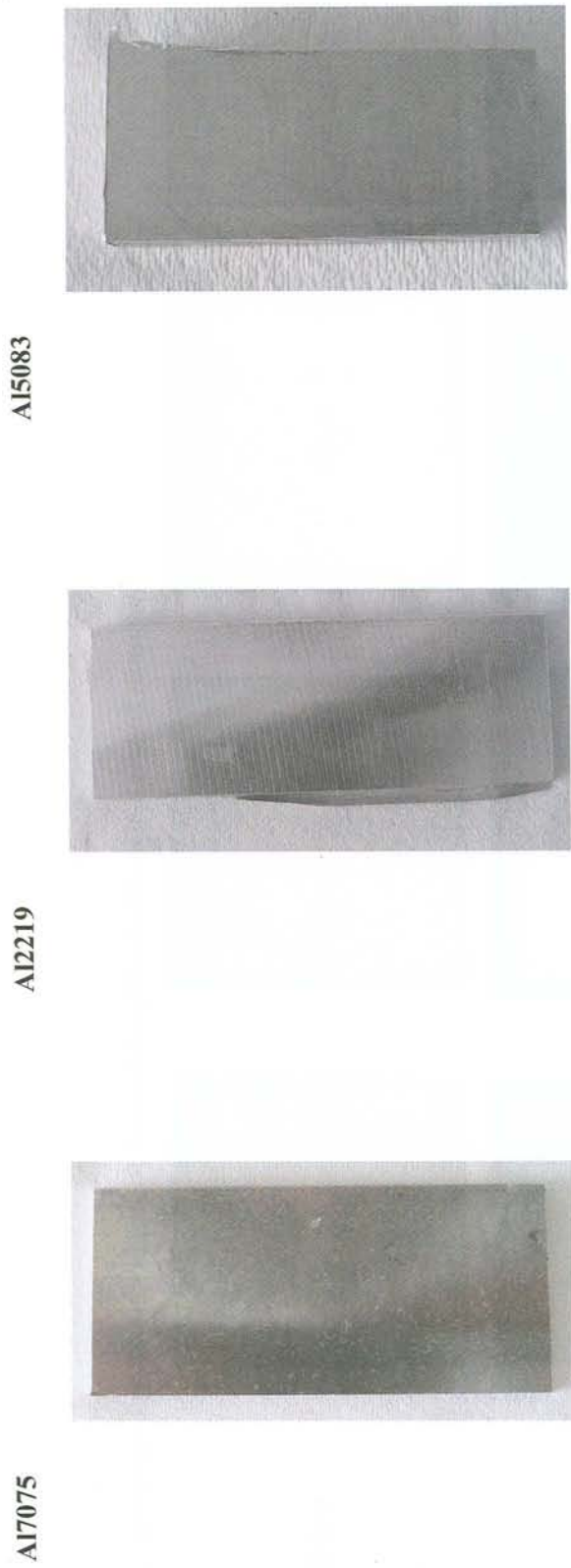


Figure 2 - Illustrative photographs of the 'as received' aluminium alloy test panels.

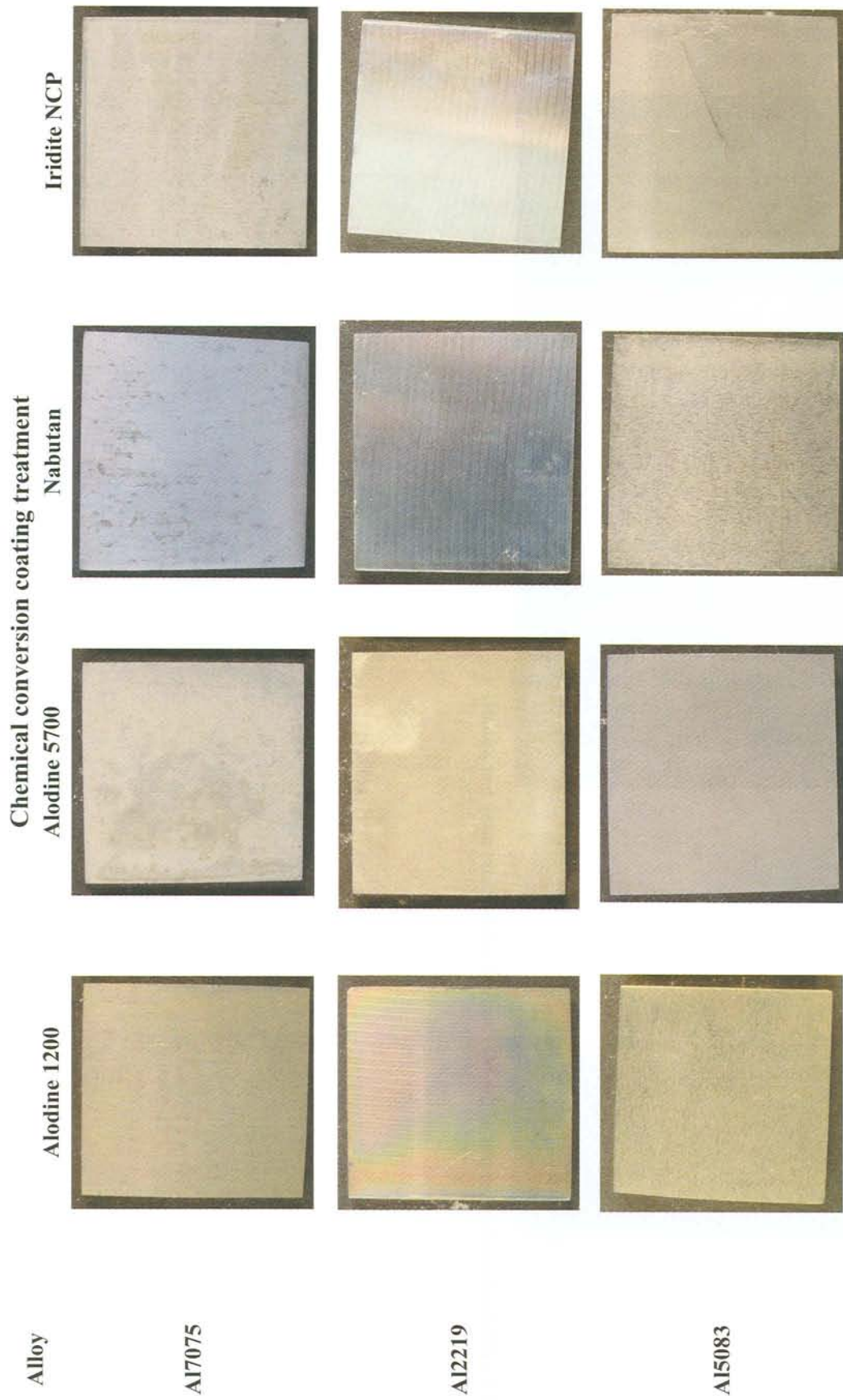


Figure 3 - Illustrative photographs of the test panels after chemical conversion coating treatment.

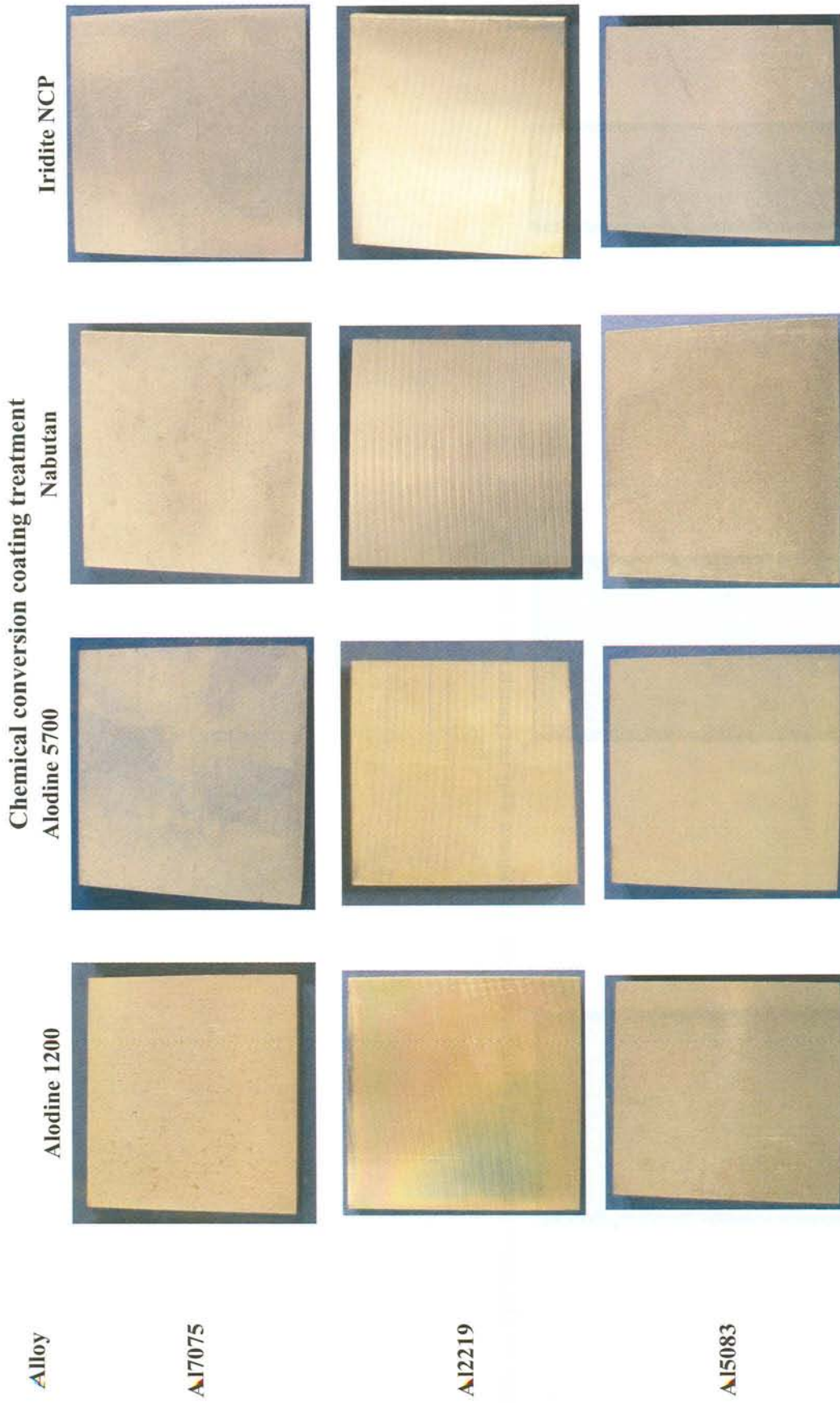


Figure 4 – Illustrative photographs of the coated test panels after thermal cycling tests.

AI5083



AI2219



AI7075



Figure 5 - Illustrative photographs of the 'as received' aluminium alloy test panels after salt spray tests.

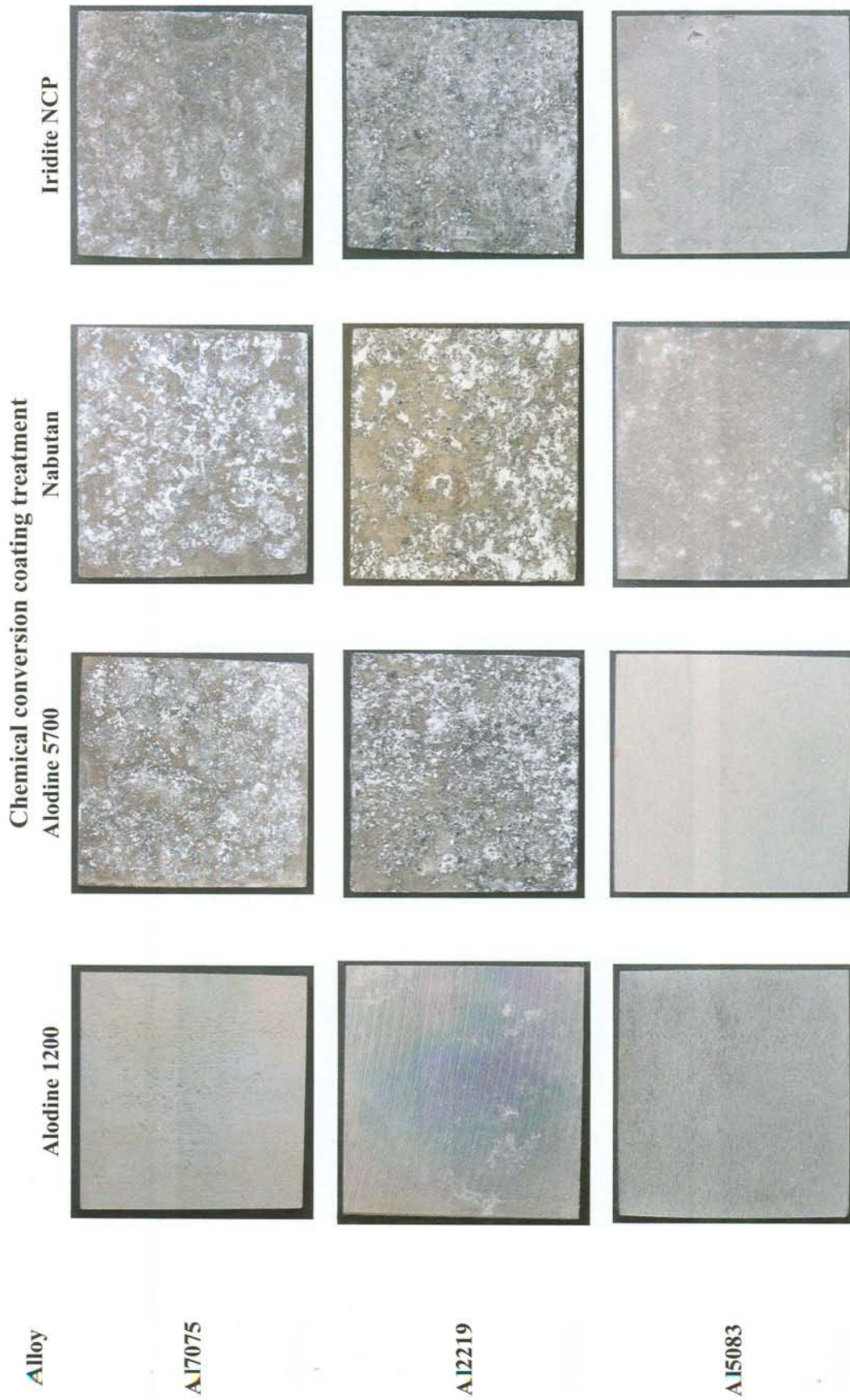


Figure 6 – Illustrative photographs of the coated test panels after salt spray tests.

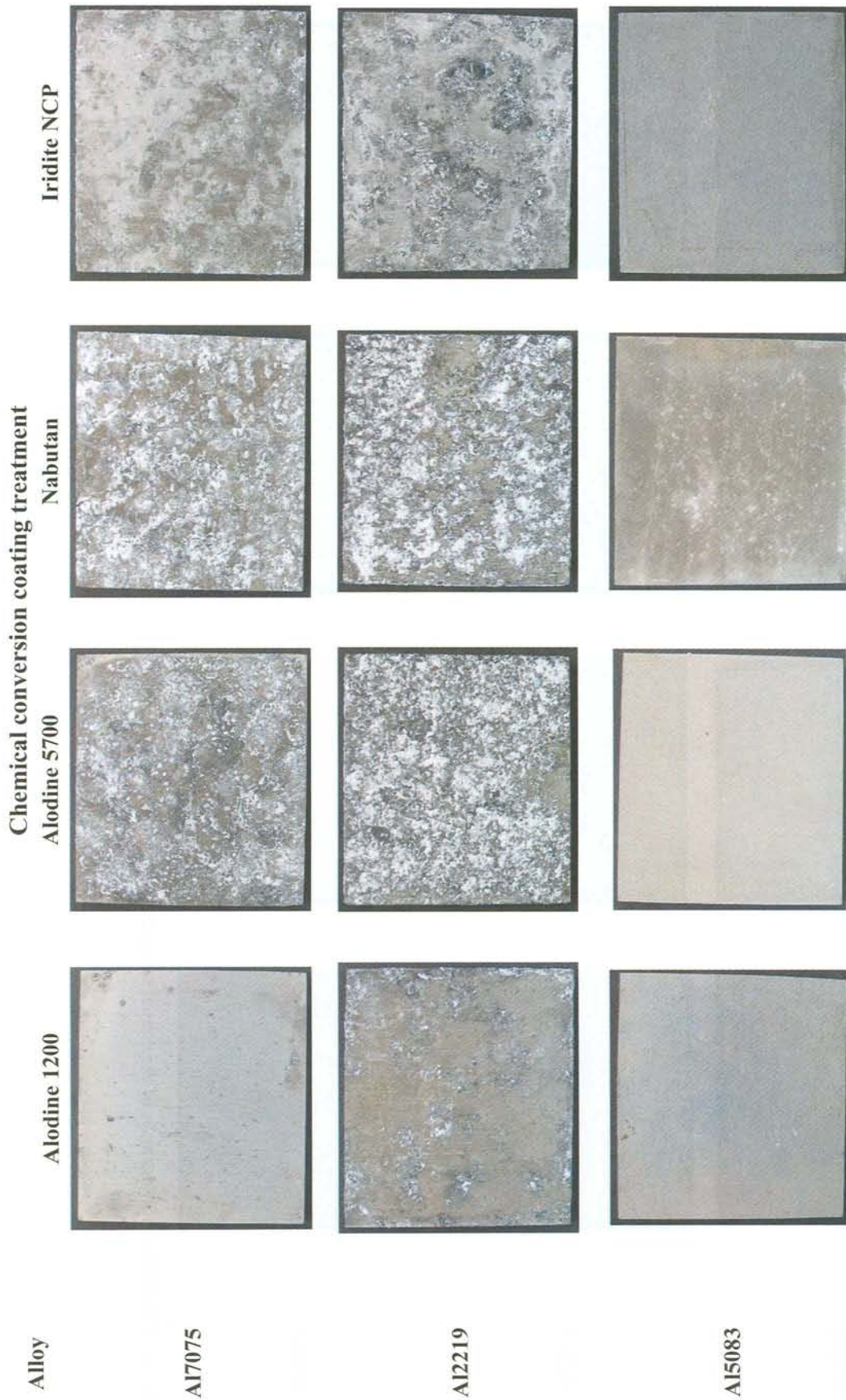


Figure 7 – Illustrative photographs of the coated test panels after thermal cycling + salt spray tests.

3.2 Surface roughness

Test specimen roughness was measured on samples at each step of the process: ‘As received’, cleaned with the Novaclean Al86 agent, coated, after thermal cycling tests, after salt spray tests, and after thermal cycling plus salt spray tests. For each test specimen, three measurements were carried out in two perpendicular directions (longitudinal and transverse) and the average results are shown in Figures 8 and 9.

In general, roughness measurements can be summarised as follows:

- a) ‘as received’ roughness is higher for Al2219;
- b) Alodine 1200 and Iridite NCP provide a higher average surface roughness for Alloys 2xxx and 5xxx. On the contrary, for Al 7xxx higher roughness was obtained for Alodine 5700 and Nabutan;
- c) A decrease in roughness was seen for all substrates after thermal cycling, as compared to the ‘as coated’ condition measurements. This evidence was probably related to the fact that after thermal cycling measurements the coated specimens exhibit a more compact and uniform surface.

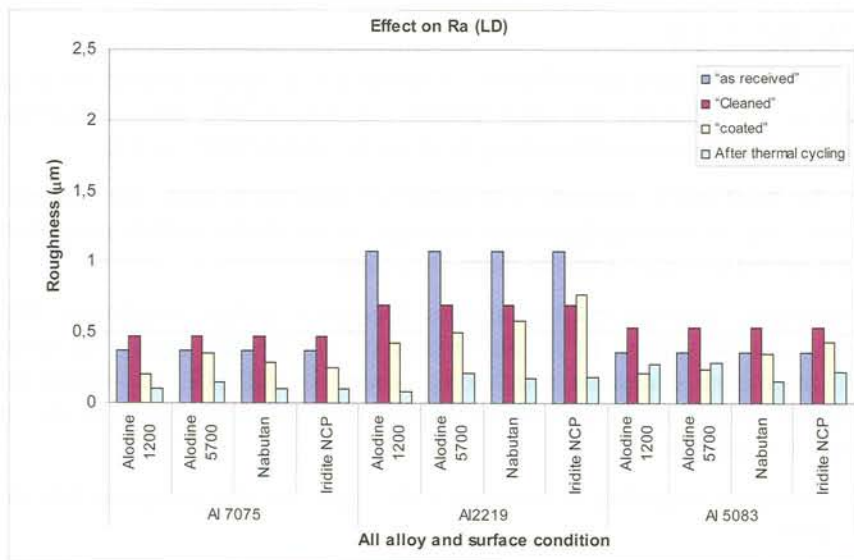


Figure 8 - Roughness measurements on the longitudinal direction.

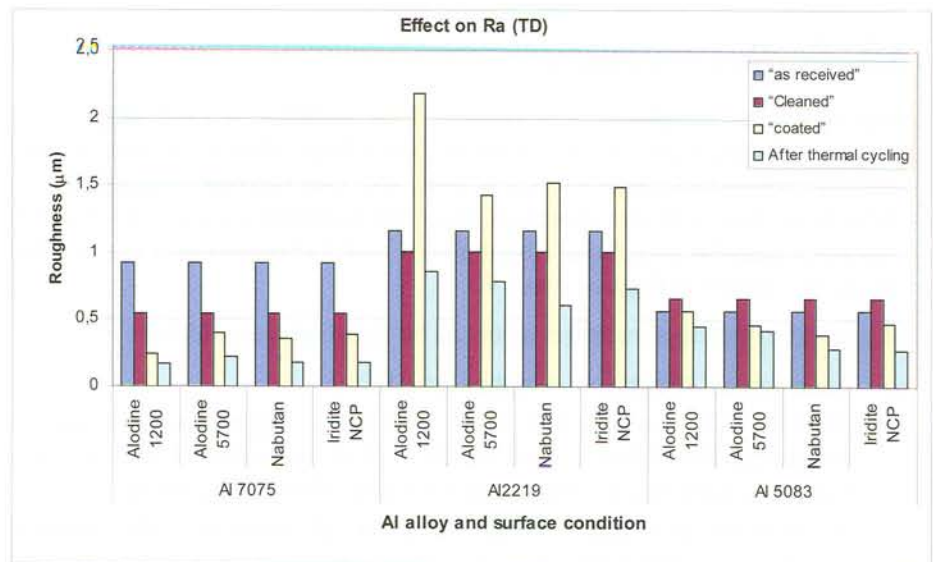


Figure 9 - Roughness measurements on the transversal direction.

For the Al7075 alloy, there is a decrease in roughness for all treatments; there is a decrease in roughness with the coating application as well as with the thermal cycling.

For the Al 5083 alloy the influence of the different surface conditions is the smallest, but it follows the same tendency as the AL7075 alloy: a decrease tendency in roughness with coating application and thermal cycling.

The Al 2219 alloy presents a decrease of roughness with the chemical cleaning but the coating deposition strongly increases the surface roughness, which decreases again with the thermal cycling.

In summary, thermal cycling always decreases surface roughness. This feature can be related to a dehydration of the surface layer. Treatment application also decreases roughness, except for Al2219, for which this treatment makes roughness values higher than those obtained in the 'as received' condition.

The behaviour described is essentially the same for the two perpendicular directions.

In general, the Al2219 test panels show a higher surface roughness than the other two aluminium alloys. It should be noted that the conversion coating treatments Alodine 1200 and Iridite NCP provide a higher average surface roughness, except for the Al7075 samples, where those coated with Alodine 5700 and Nabutan showed higher values.

The surface roughness measurements after the salt spray tests were only performed on the test panels treated with the Alodine 1200S and on samples of Al5083, since that in general the surface of samples presented visible evidence of corrosion to allow the measurement of the roughness. In those samples measured it can be seen that there is no significant differences between the roughness values obtained after salt spray tests.

3.3 Surface electrical resistivity measurements

The surface resistivity of the test specimens was measured for the samples 'as produced', at 200 cycles of the thermal cycling test. Once again, these measurements were not performed on test panels after salt spray exposure, since in general the surface was attacked. For each test specimen /

conversion coating treatment, 10 measurements were carried out. Figure 10 summarises the average results obtained.

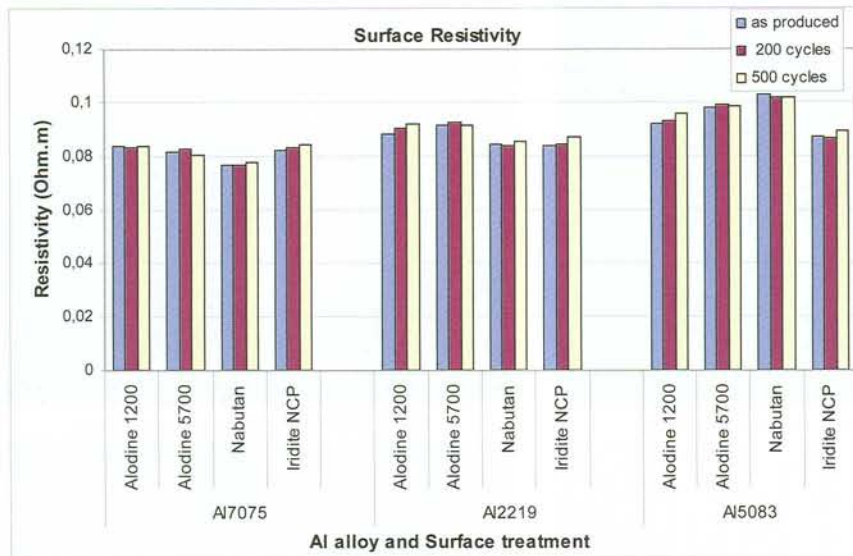


Figure 10 – Surface electrical resistivity measurements of test panels.

In general, the surface electrical resistivity of all test panels 'as produced' is very similar for all the chemical conversion treatments under evaluation and did not suffer significant change after the thermal cycling tests, if the experimental standard deviation is considered.

3.4 Surface morphology analysis - Scanning electron microscopy

3.4.1 After cleaning with Novaclean Al86

Figure 11 illustrates the SEM micrographs of Al2219 and Al7075 specimens, after cleaning with *Novaclean Al86*. Samples presented higher roughness before the cleaning step, and some dirt was eliminated in this step.

The remaining particles on the surface were secondary phases from the corresponding aluminium alloy. This was confirmed by chemical analysis by SEM/EDX. Some holes can also be seen on the surface; this is attributed to the mechanical removal of the secondary phases, either during material processing or selective leaching of secondary phases by the cleaning agent.

No cleaning test was performed on the Al5083 samples, due to insufficient material quantities.

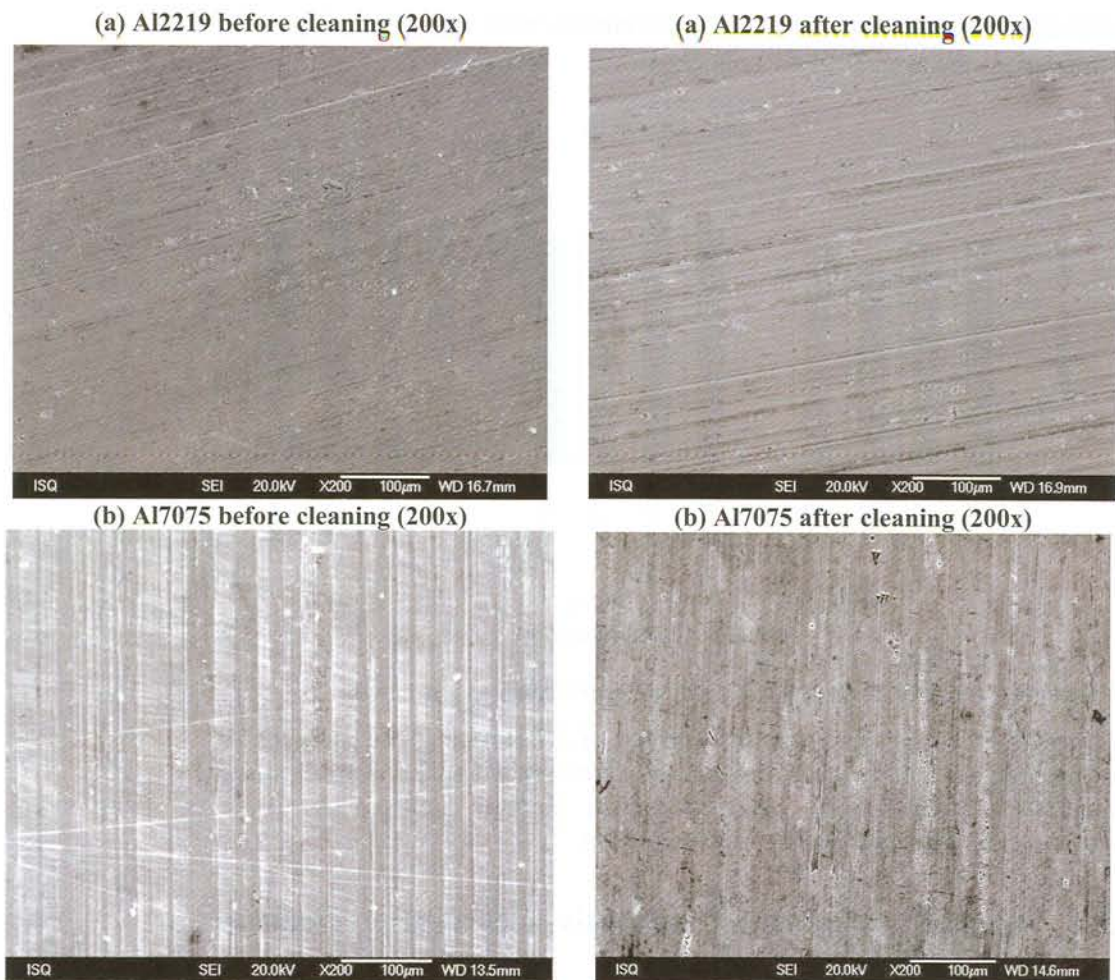


Figure 11 - SEM micrographs of Al2219 and Al7075 specimens before and after cleaning with *Novaclean Al86*.

3.4.2 After chemical conversion coating treatments

Figures 12 to 14 show the secondary electron photomicrographs of the coated test panels. The EDS spectra correspondent for each chemical conversion coating were stored.

Apart from the Alodine 5700, SEM observation showed relatively uniform, closed coatings for all the treatments tested. Discontinuities found on the surface can be related to previous surface defects or microstructural heterogeneities induced by the secondary phases. In fact, it is expected that varying substrate composition and reactivity presented by the three alloys (Al7075, Al2219 and Al5083) will influence the formation of the surface films.

EDS analysis revealed that these morphological heterogeneities are also coated, making the coating a continuous film over the complete alloys surfaces.

The Alodine 5700 coating peeled off in significant areas of the Al7075, a stronger attachment being observed on Al2219 surfaces. This peeling off can be interpreted by a poor adhesion to the substrate or internal stresses of the coating or a combination of both of these effects. In the Al5083 alloy, on the contrary, this treatment formed a compact film (Figure 13). EDS spectra revealed the presence of F, Ti, Zr, O and C, along with the alloying elements characteristic of the alloys under study (all results and images have been stored electronically for further reference).

In an attempt to overcome the poor adhesion of Alodine 5700 on Al7075 and Al2219 alloys, coating tests were performed with varying immersion times (30 seconds, 1, 3 and 5 minutes), with all other parameters kept constant. The corresponding morphologies are illustrated in Figures 15 to 16. For the Al2219 alloy, the best result was obtained for 3 minutes immersion, while for the 7075 alloy the best result was obtained for 1 minute immersion. Nevertheless, the surfaces were very similar to those obtained previously, in terms of morphology and composition. Furthermore, it was possible to observe that the surface was probably composed of two coating layers: one more superficial and the other beneath.

SEM observation shows that films formed on the test panels are probably thin. In fact, it must be emphasised that some defects were present in coatings, probably related with the secondary phase distribution over the surface.

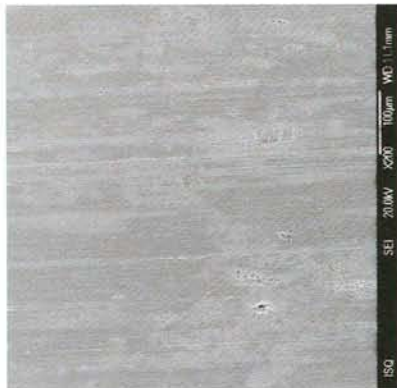
SEM images of the test panels coated with the Alodine 1200S treatment show a typical mud-cracked surface morphology and are very similar for all the aluminium alloys. It was possible to identify some black spots over the surface, which indicates that the coating did not cover the whole surface of the sample. These sites are supposed to be related to intermetallic particles presented on the surface of these alloys, suggesting that the thickness of the coating is less on top of these particles. The same mud-crack surface morphology has been observed by other authors [23], in a study performed on chromium conversion coating Al7075 alloys.

The semi-quantitative analysis of the chemical elements reveals the presence of some constituents of the aluminium alloys and elements that proceed from the conversion chemical coating, mainly: Cr, F, Zr and O. However, due to the limitations of this technique, namely the inability to analyse light elements, the percentage of O cannot be considered in a reliable quantitative way.

The surface morphology of test panels coated with the Nabutan and Iridite NCP showed a uniform surface, nevertheless some black holes existed on the surface, suggesting that the coating did not cover the whole surface of the samples. The EDS analysis identified that the treated layers are formed mainly by F, Ti, O for the Nabutan treatment. F, P, Ti and O plus the elements of each alloy were associated with the Iridite NCP treatment. Once again, the percentage of O cannot be considered in a quantitative form.

Chemical conversion coating

**Alodine 1200
(200X)**



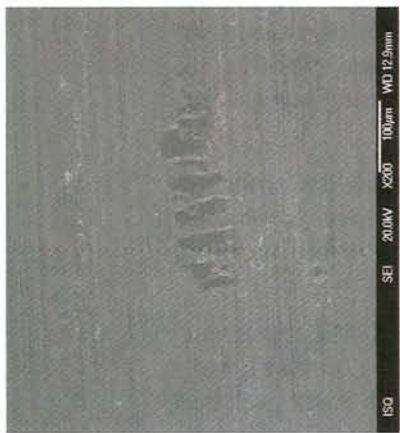
**Alodine 5700
(200X)**



**Nabutan
(200X)**



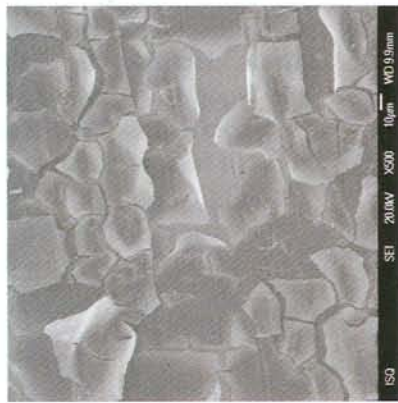
**Iridite NCP
(200X)**



(1000X)



(500X)



(1000X)



(1000X)

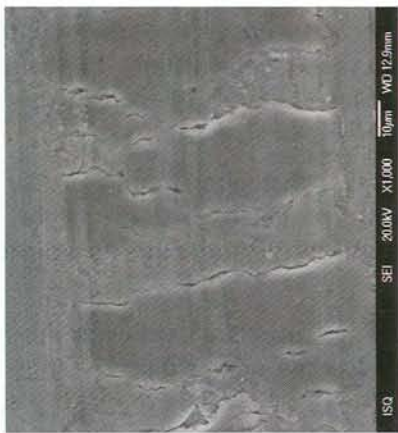
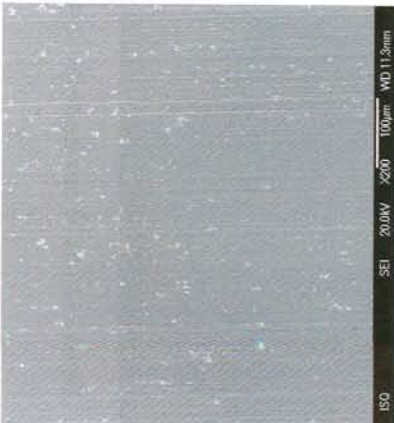


Figure 12 - SEM micrographs of the test panels Al7075 after chemical conversion coating treatments.

Chemical conversion coating

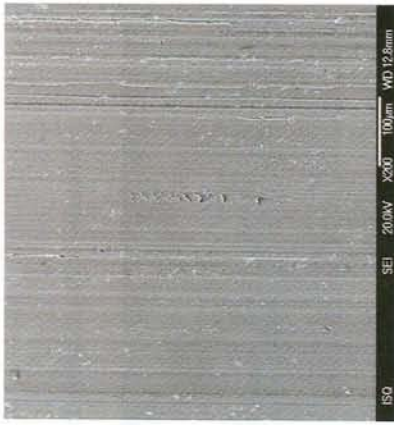
**Alodine 1200
(200X)**



**Alodine 5700
(200X)**



**Nabutan
(200X)**



**Iridite NCP
(200X)**



(1000X)



(550X)



(1000X)



(1000X)



Figure 13 - SEM micrographs of the test panels Al2219 after chemical conversion coating treatments.

Chemical conversion coating

**Alodine 1200
(200X)**



**Alodine 5700
(200X)**



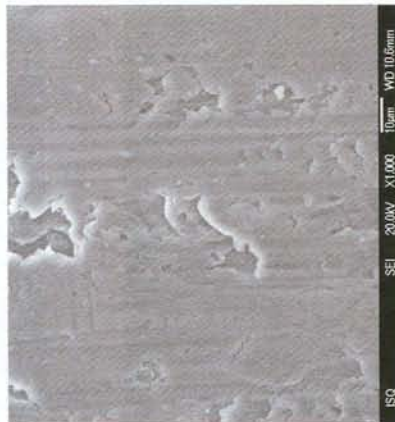
**Nabutan
(200X)**



**Iridite NCP
(200X)**



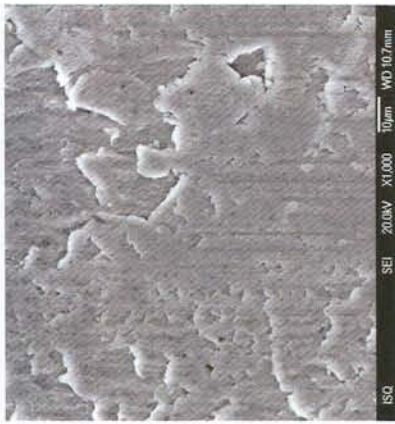
(1000X)



(1000X)



(1000X)



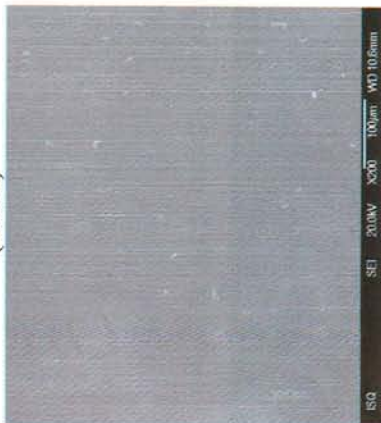
(1000X)



Figure 14 - SEM micrographs of the test panels AI5083 after chemical conversion coating treatments.

Chemical conversion coating - Alodine 5700

**30 sec.
(200X)**



(1000X)



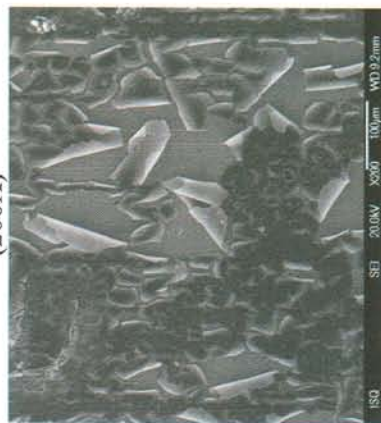
**1 min.
(200X)**



(1000X)



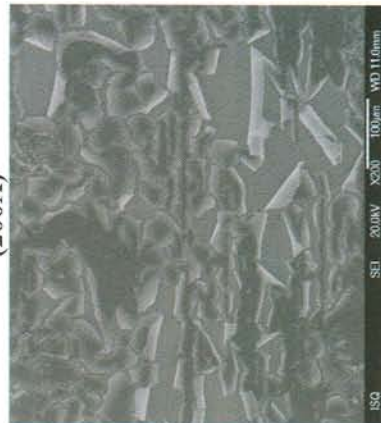
**3 min.
(200X)**



(1000X)



**5 min.
(200X)**



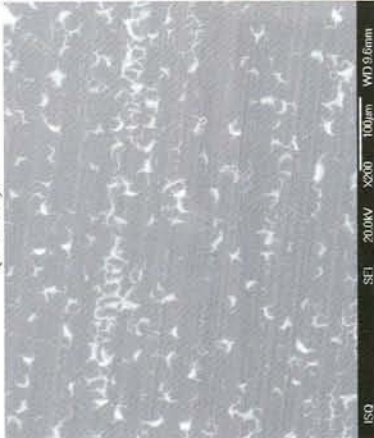
(1000X)



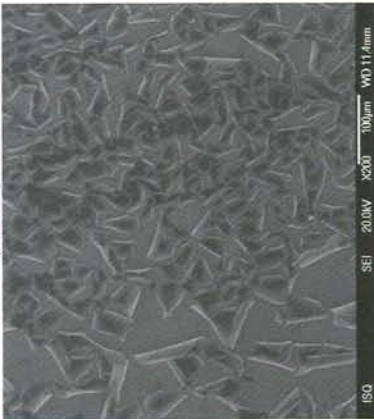
Figure 15 - SEM micrographs of the test panels A17075 after chemical conversion coating treatment with Alodine 5700 at different times of immersion.

Chemical conversion coating - Alodine 5700

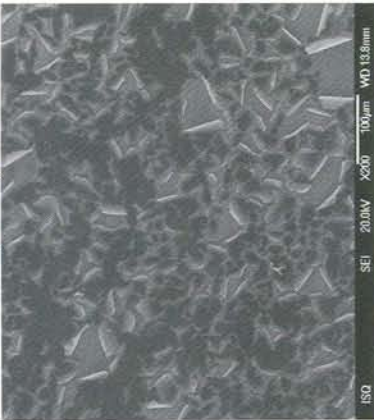
30 sec.
(200X)



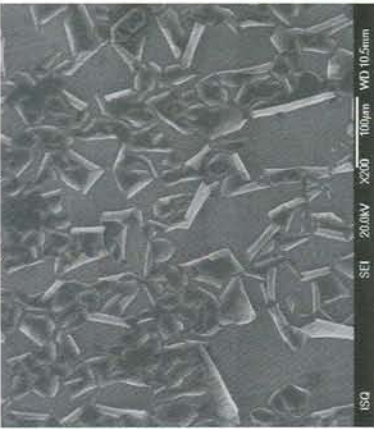
1 min.
(200X)



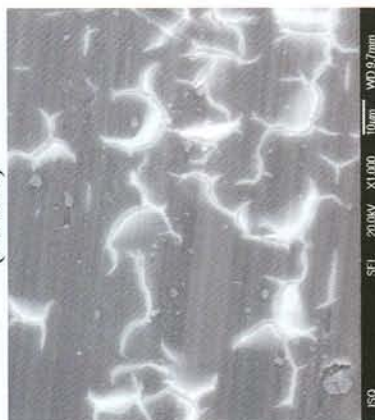
3 min.
(200X)



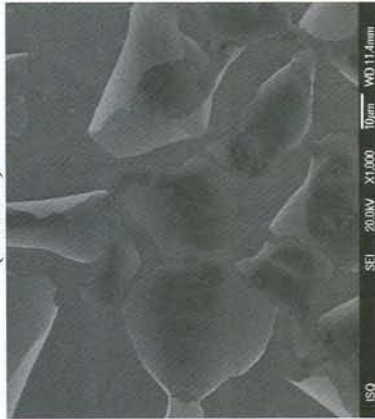
5 min.
(200X)



(1000X)



(1000X)



(1000X)



(1000X)



Figure 16 - SEM micrographs of the test panels Al2219 after chemical conversion coating treatment with Alodine 5700 at different immersion times.

3.4.3 After thermal cycling tests

SEM observation after the thermal cycling tests revealed minor changes in the morphology of all coated surfaces except for the Al7075 and Al2219 (Figures 17 to 19). This was more evident in test panels coated with Alodine 1200 and Alodine 5700. In effect, the comparison of SEM images before and after thermal cycling shows clearly that, after thermal cycling, the coated specimens exhibit a more compact and uniform surface. For Al7075 and Al2219, the non (poor)-adherent bits of the coatings observed in the 'as deposited' condition were absent after thermal cycling. This is coherent with lack of adherence to the substrate, and the thermal stress induced by the temperature cycling promoted the complete peel-off of the non-adherent films parts.

All these results support surface roughness measurements, which revealed a decrease in R_a after the thermal cycling test.

The representative EDS spectra have been retained at ISQ.

The dark areas observed on the coated samples surfaces are related with the coating layer formed, while the white area corresponds to the surface where the coating treatment had poor adhesion to the substrate, which is confirmed by energy dispersive spectroscopy (EDS) analysis. This fact was more evident on samples Al7075 and Al2219 submitted to the Alodine 5700 treatment. The test panels treated with Nabutan and Iridite NCP were relatively unaffected by the thermal cycling tests.

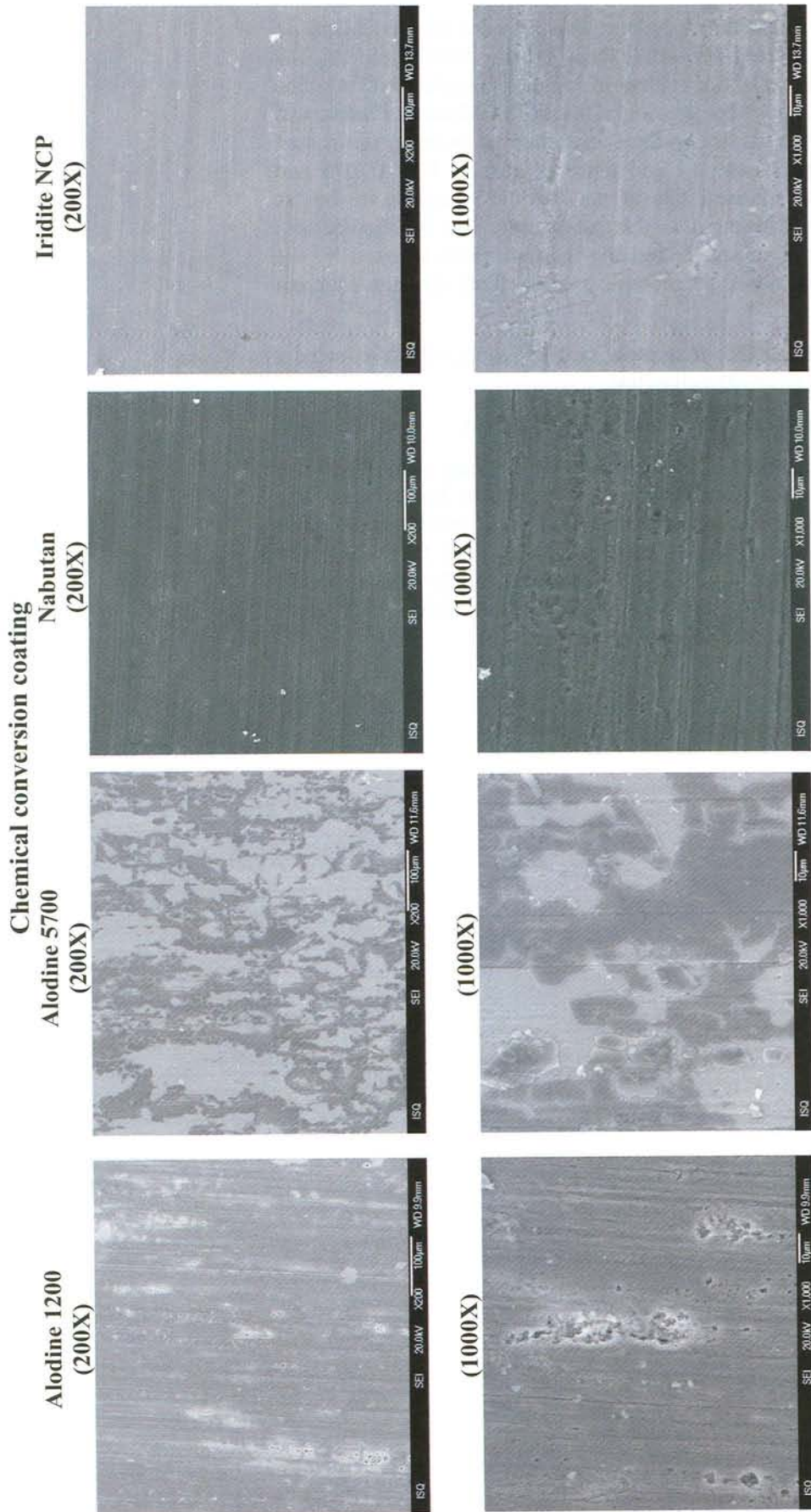
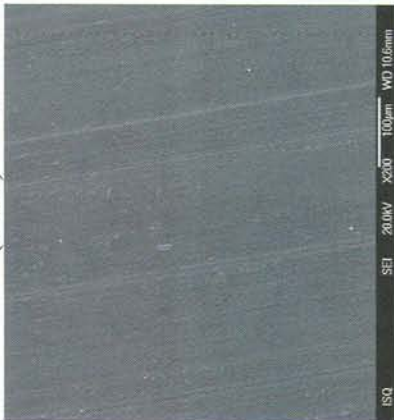


Figure 17 – SEM micrographs of the coated test panels Al7075 after thermal cycling tests.

Chemical conversion coating

Alodine 1200
(200X)



Alodine 5700
(200X)



Nabutan
(200X)



Iridite NCP
(200X)



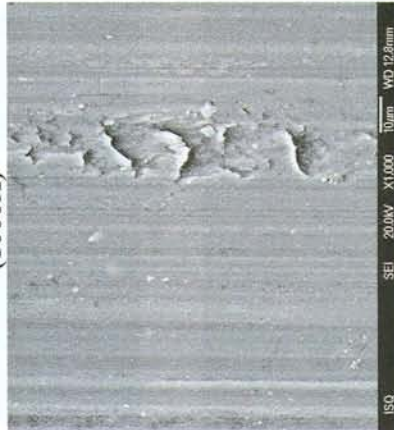
(1000X)



(1000X)



(1000X)



(1000X)



Figure 18 – SEM micrographs of the coated test panels Al2219 after thermal cycling tests.

Chemical conversion coating

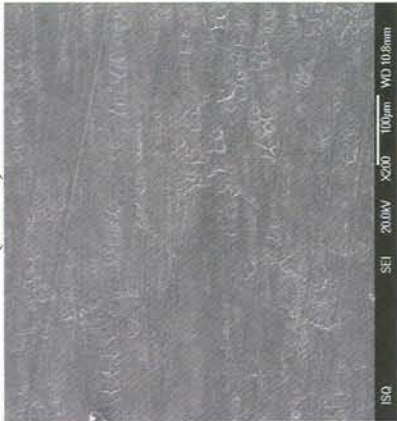
**Alodine 1200
(200X)**



**Alodine 5700
(220X)**



**Nabutan
(200X)**



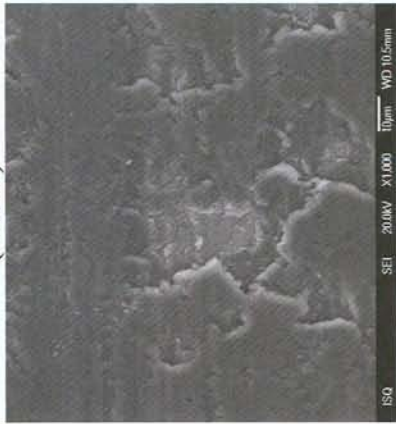
**Iridite NCP
(200X)**



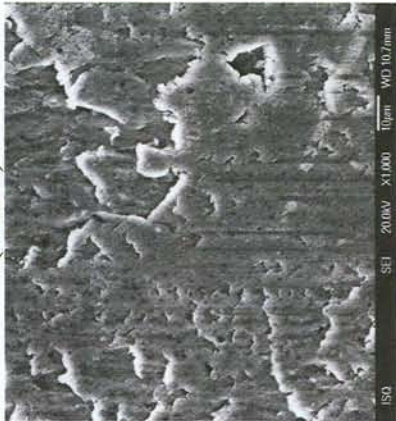
(1000X)



(1000X)



(1000X)



(1000X)



Figure 19 – SEM micrographs of the coated test panels Al5083 after thermal cycling tests.

3.4.4 After salt spray tests

The evaluation of samples after salt spray exposure by SEM revealed that Alodine 1200S coated samples had a similar surface morphology to the 'As produced' samples. Nevertheless, the mud-cracked surface appearance was not so evident, except for samples from Al2219. The semi-quantitative analysis of the chemical elements identified the constituents of the aluminium alloys, as well as elements that proceed from the conversion chemical coating and a small percentage of Na.

In general, SEM observation of the test panels Al7075 and Al2219 treated with the three chemical conversion coatings under study, showed that the surface morphology is formed by a 'white' corrosion product, mainly composed of Al, O, Na and the elements of each alloy, indicating Al substrate degradation and sodium chloride residues.

The Al5083 test panels exposed to salt spray did not present evidence of corrosion, even after 7 days of exposure. SEM images of these test panels showed an unaffected surface morphology, although a small amount of white corrosion product could be observed. The EDS analysis identified the elements revealed before the exposure, with an increase in O percentage and the presence of a small percentage of Na.

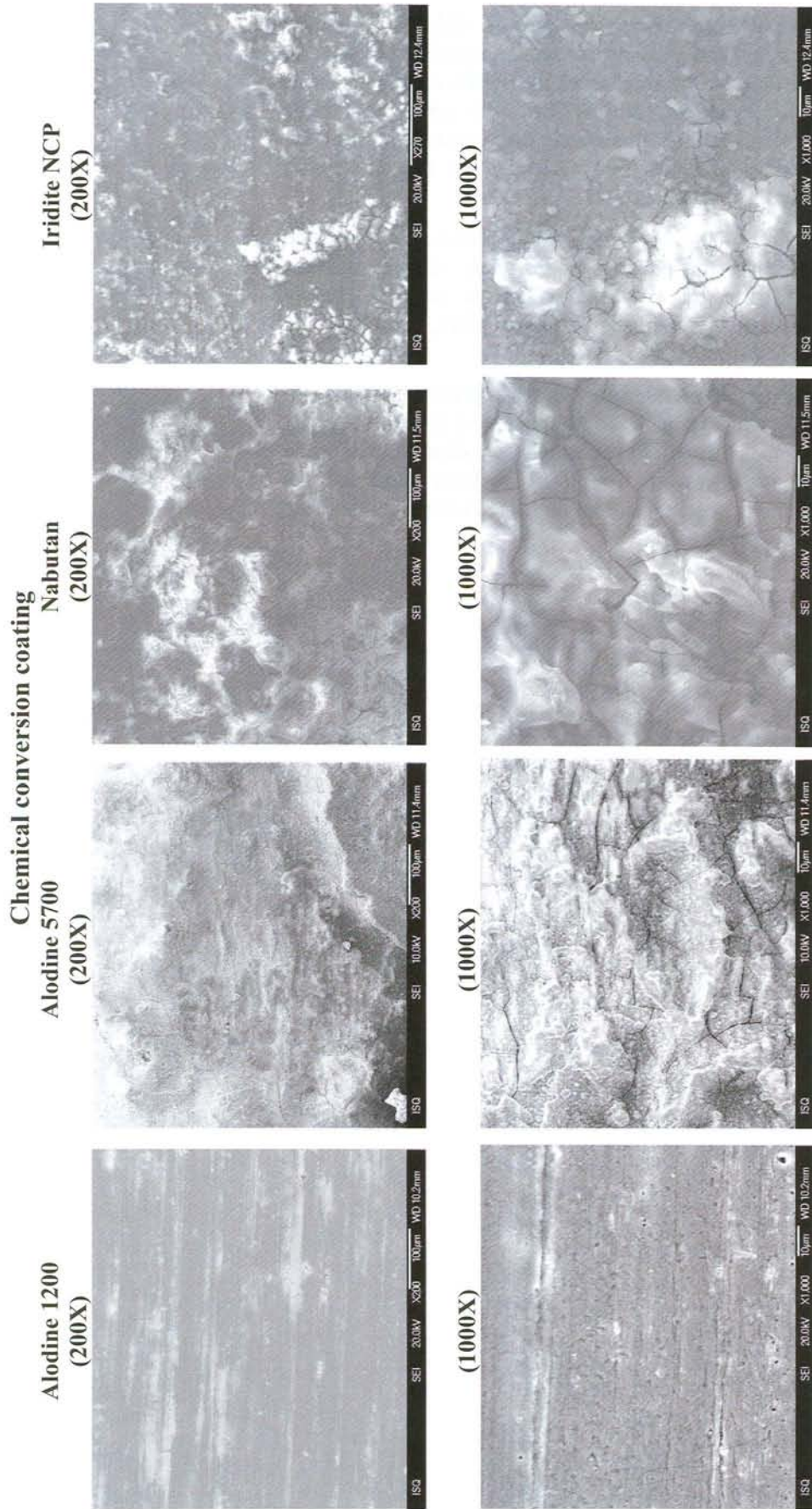


Figure 20 – SEM micrographs of the coated test panels Al7075 after salt spray tests.

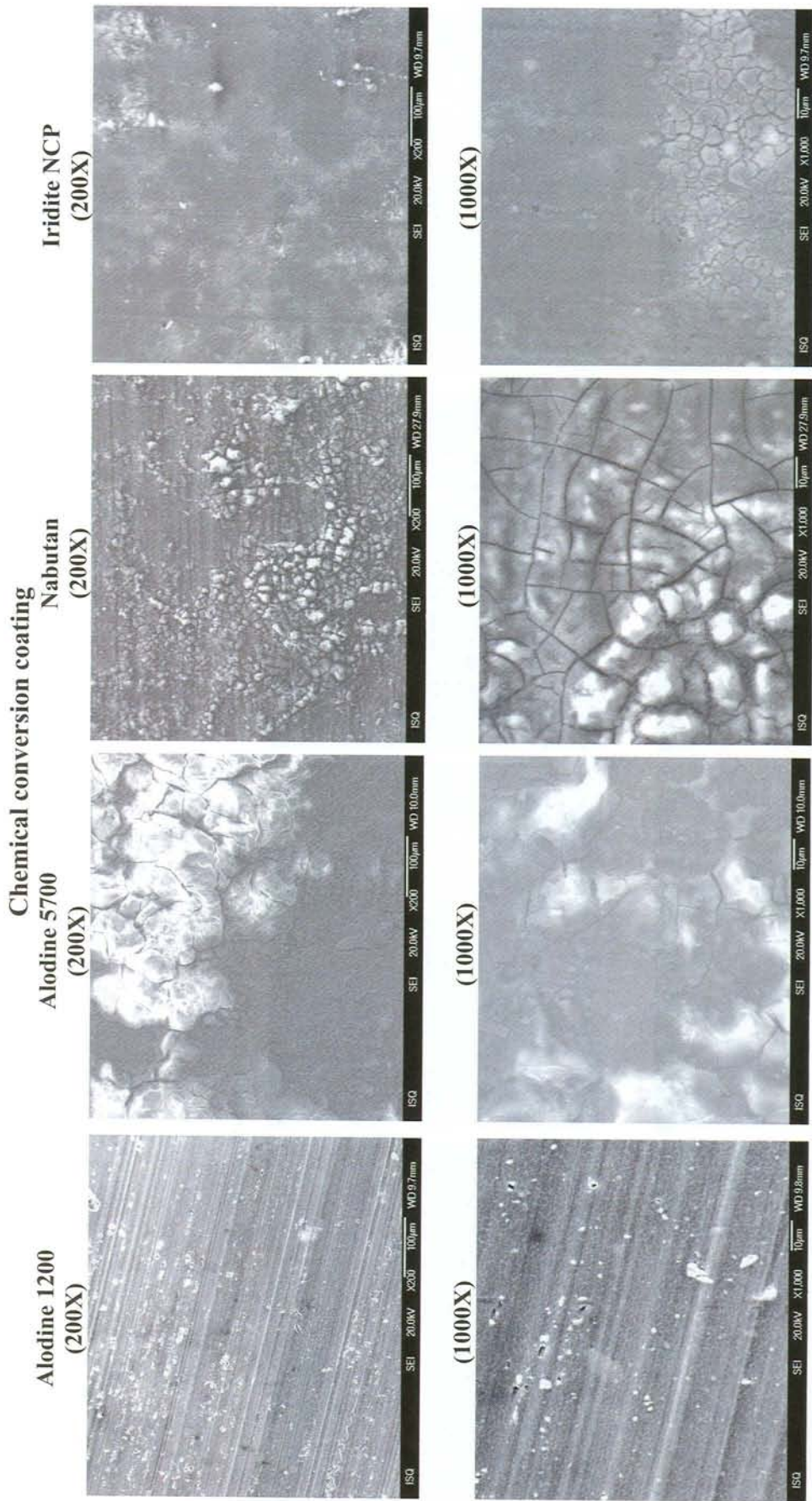


Figure 21 – SEM micrographs of the coated test panels Al2219 after salt spray tests.

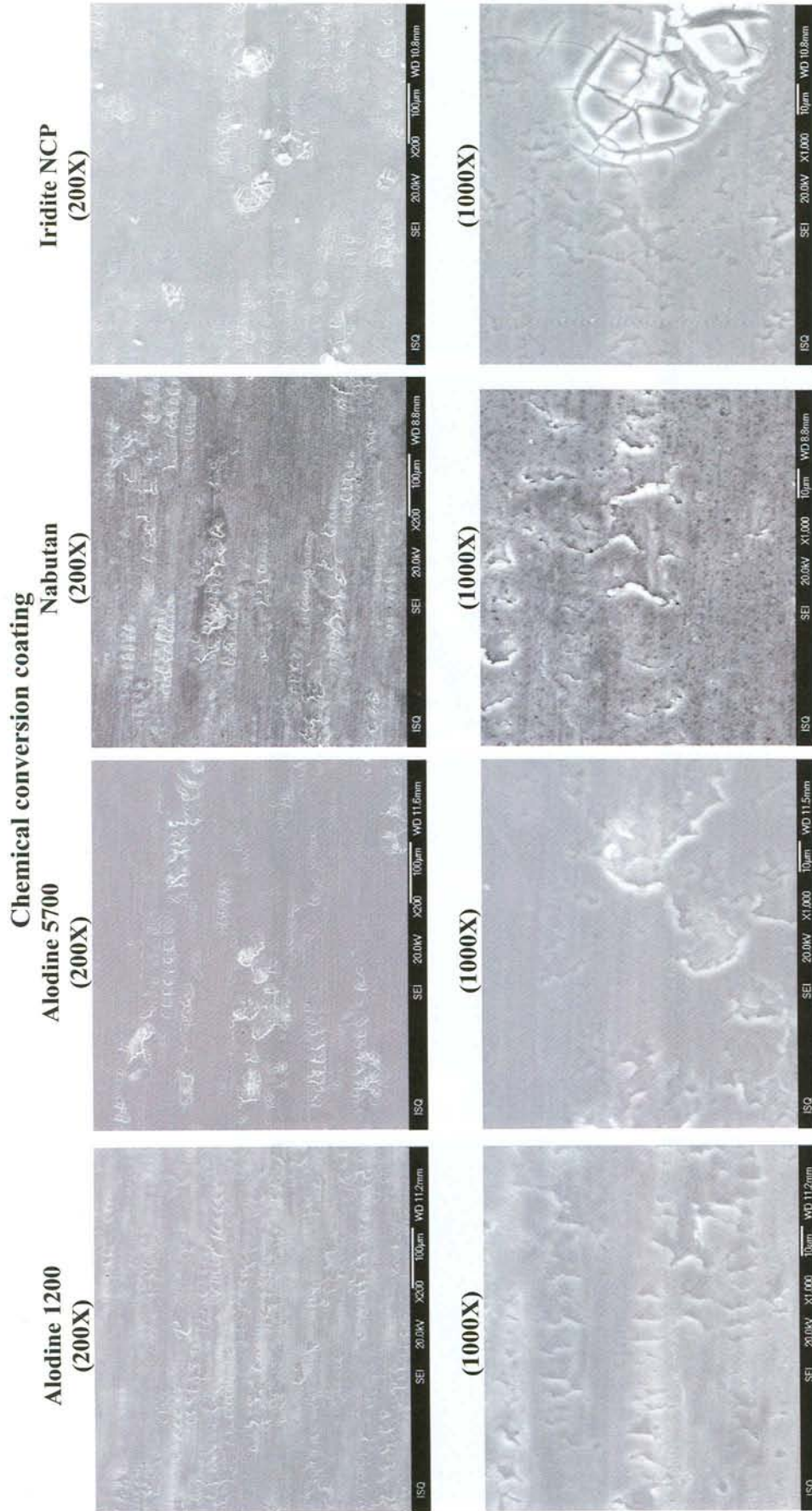


Figure 22 – SEM micrographs of the coated test panels Al5083 after salt spray tests.

3.4.5 After thermal cycling plus salt spray tests

On the whole, SEM observation of the test panels that were submitted to thermal cycling followed by salt spray exposure brought out changes in the morphology of all coated surfaces quite similar to those obtained after the salt spray exposure.

Once again, Al5083 samples showed no signs of corrosion for all treatments studied.

The surface morphology of test panels from the other two treated aluminium alloys revealed an equivalent morphology to those obtained before. The surfaces were covered with a layer of white corrosion products, formed mainly of Al, O, Na and other constituents of the aluminium substrates.

In summary, sample exposure to thermal cycling did not introduce significant changes on the corrosion behaviour.

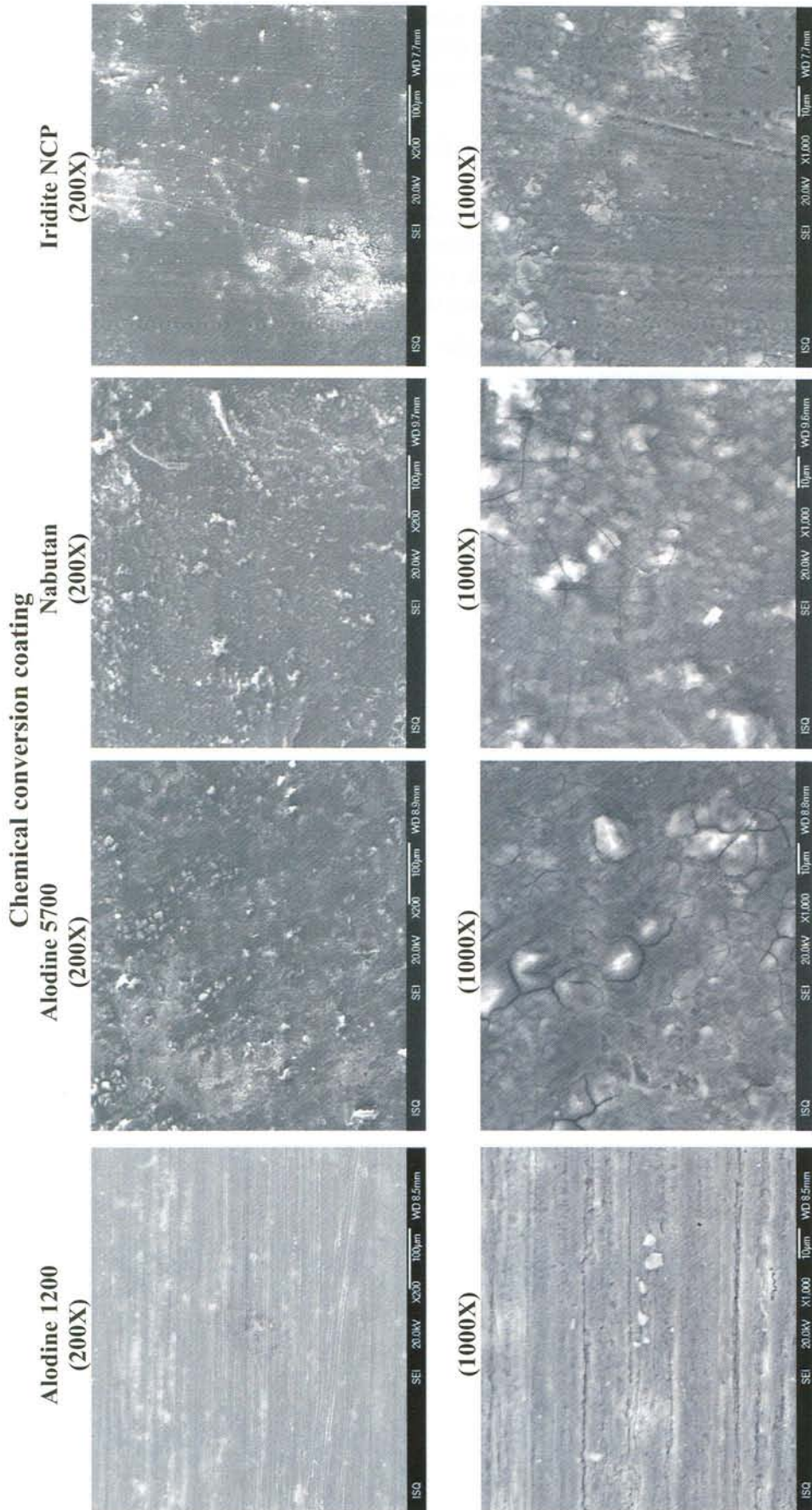


Figure 23 – SEM micrographs of the coated test panels Al7075 after thermal cycling + salt spray tests.

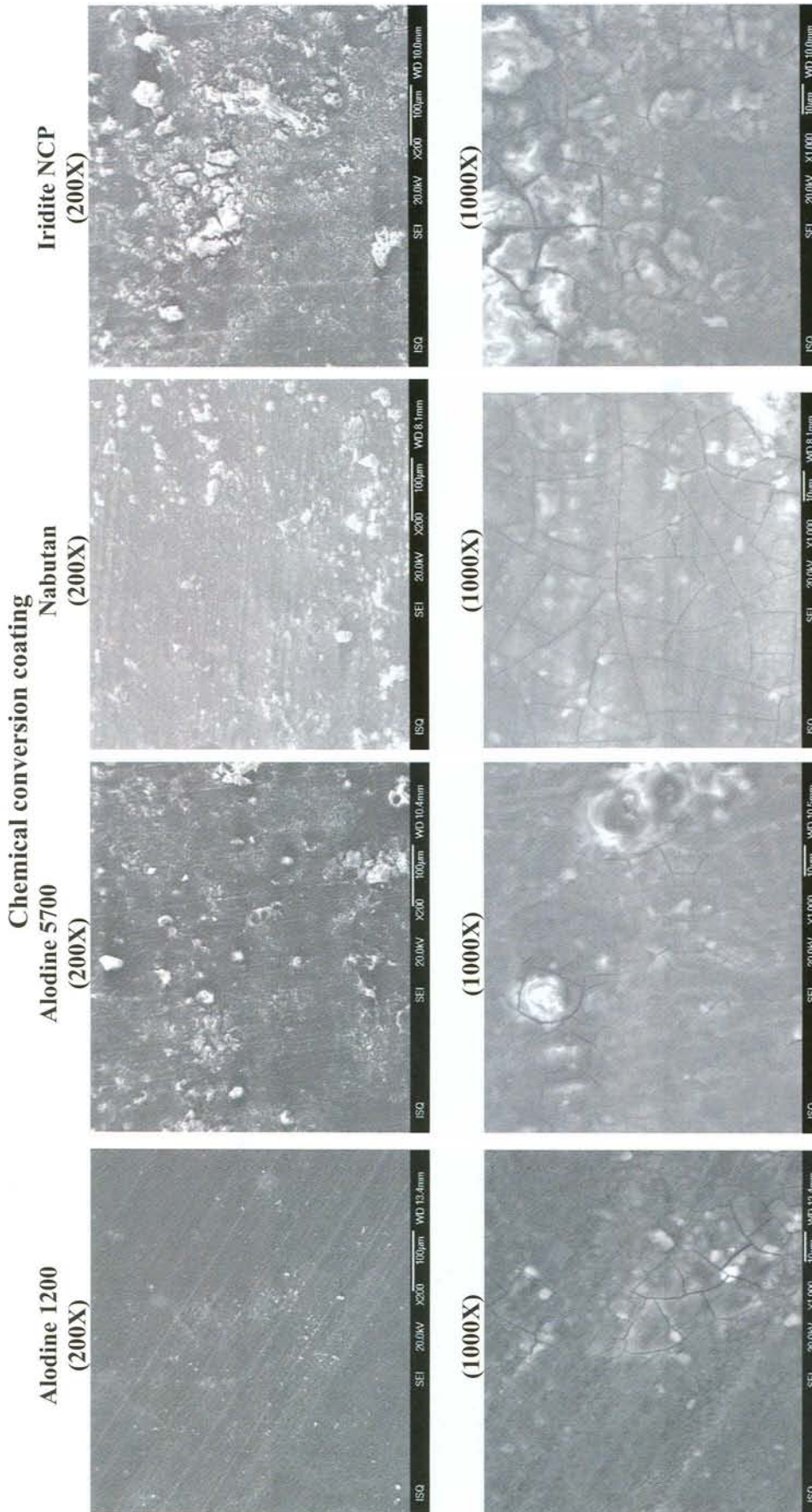


Figure 24 – SEM micrographs of the coated test panels A12219 after thermal cycling + salt spray tests.

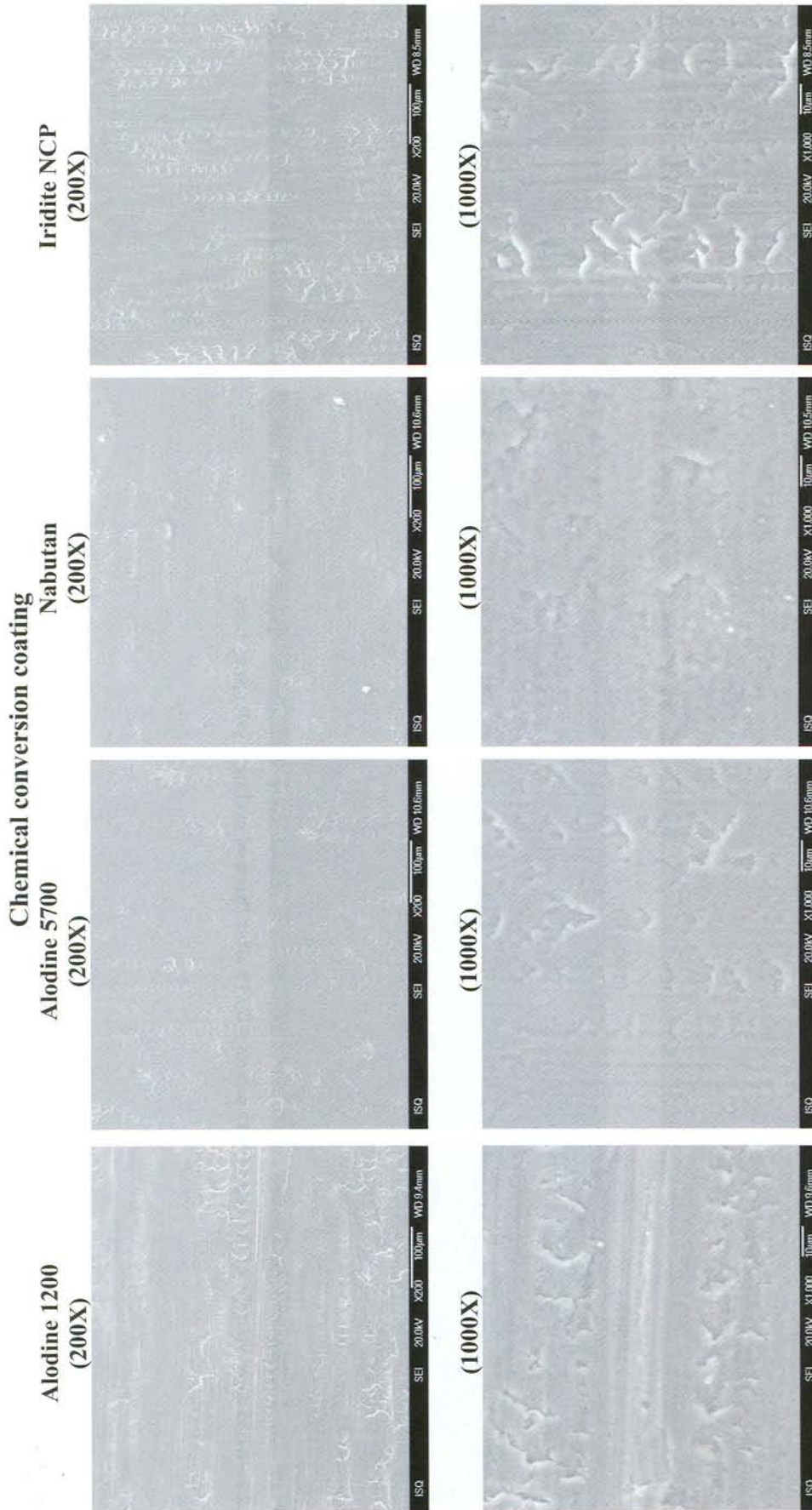


Figure 25 – SEM micrographs of the coated test panels AI5083 after thermal cycling + salt spray tests.

3.4.6 Comparison and correlation between Aluminium alloys and techniques performed

Tables 5 to 7 summarise the results obtained for each aluminium alloy and characterisation performed.

Al7075

Generally, the surface roughness of test panels treated with the four conversion chemical coatings was very similar. However, for Alodine 5700 and Nabutan coated samples, the values were slightly higher. It should be noted that there was a decrease in roughness values for all treatments after coating application, as well as after the thermal cycling. This feature can be related, on one side to the chemical etching performed by the cleaning agent and coating deposition and on the other side, to the fact that after thermal cycling the coated specimens exhibited a more compact and uniform surface, probably due to surface layer dehydration and spalling of poor-adherent coated areas.

The surface electrical resistivity of all test panels 'as produced' was very similar for all the chemical conversion treatments under evaluation, and did not suffer significant changes after thermal cycling.

Alodine 1200S treated samples showed a typical mud-cracked surface morphology, and semi-quantitative analysis of the chemical elements revealed the constituents of the aluminium alloy, as well as elements that proceed from the conversion chemical coating. The Alodine 5700 coating morphology developed on the surface test panel exhibited a surface where the coated layer is not continuous, indicating a poor substrate adhesion. The EDS spectra on the coated layer revealed the presence of elements characteristic of the chemical coating and Al7075 alloy. The surface morphologies of the Nabutan and Iridite NCP coated test panels showed uniform surfaces.

After thermal cycling, the coated specimens display a compacter and more uniform surface, and the morphology in terms of the elements constituents of the coating layer appears to be quite similar. This was more evident in Alodine 5700 coated test panels since the thermal stress induced by the temperature cycling promoted the complete peel-off of the non-adherent films areas.

After the salt spray tests, except for Alodine 1200S treated samples, the surface morphologies are covered by a layer of 'white' corrosion products.

Al2219

Al2219 test panels present higher initial surface roughness, a roughness decrease could be observed after chemical cleaning. However, the coating deposition strongly increases the surface roughness, which decreases again after thermal cycling, probably related to surface layer dehydration. The Alodine 1200 and Iridite NCP conversion coating treatments provide higher average surface roughness.

The electrical surface resistivity of all 'as produced' test panels were very similar for all the chemical conversion treatments under evaluation, and did not suffer significant changes after the thermal cycling.

Alodine 1200S coated samples present a typical mud-cracked surface morphology, and the surface is mainly composed of elements from the alloy and from the chemical conversion treatment. The Alodine 5700 coating **peeled off in significant areas of the Al2219 surface, which can be**

interpreted as a poor adhesion to the substrate or internal stresses of the coating, or a combination of both of these effects. On the other hand, the surface morphology of test panels coated with the Nabutan and Iridite NCP showed a uniform surface.

After thermal cycling, the coated samples showed a compacter and more uniform surface, and the morphology of the coating layer in terms of the elements constituents was very similar. This was more clearly seen in Alodine 5700 coated test panels since the thermal stress induced by the temperature cycling promoted the complete peel-off of the non-adherent film areas. In Nabutan and Iridite NCP treated test panels, it could be seen that they were roughly unaffected by the thermal cycling.

After the salt spray tests, except for Alodine 1200S coated test panels, surfaces exhibit a white corrosion product layer.

Al5083

Al5083 alloy showed the same influence of different surface conditions, but it followed the same tendency as the Al7075 alloy: roughness decrease with coating application and thermal cycling.

In general, surface roughness and surface electrical resistivity of all test panels 'as produced' were very similar for all the chemical conversion treatments under evaluation, and did not suffer significant changes after thermal cycling.

Coated specimen surface morphologies displayed a compacter and more uniform coating. Furthermore, Alodine 5700 treated samples did not present the lack of substrate adhesion observed on samples of Al7075 and Al2219 alloys.

Thermal cycling did not significantly affect sample surface morphologies; however they exhibited a more compact surface after cycling. The coating layers were composed essentially of the same elements: element constituents of the aluminium alloy and those that provided for the chemical conversion treatment.

After the salt spray tests, there was no evidence of corrosion on the Al5083 coated samples after 7 days of exposure, for each of the treatments studied.

Table 5 – Results obtained for Al7075 test panels.

| Chemical conversion coating | 'As received' | | | 'As produced' | | | | TC | | SS | | TC + SS |
|-----------------------------|---|------------------------------|----------------|---|-------------------------------|--|---|-------------------------------|----------------------|--|--|---------|
| | SEM | Roughness | Resistivity | SEM | Roughness | Resistivity | SEM | Roughness | Resistivity | Visual Analysis | Visual Analysis | |
| Alodine 1200S | | | | - uniform coating; - typical mud-cracked surface morphology; - black spots on surface | - surface roughness decreases | | - more compact and uniform surface | - surface roughness decreases | | - no evidence of corrosion | - no evidence of corrosion | |
| Alodine 5700 | - The remaining particles on surface were secondary phases from the corresponding aluminium alloy | - relative surface roughness | - not measured | - coating peeled-off; - poor adhesion to substrate | - higher surface roughness | - surface electrical resistivity is very similar | - complete peel-off of the non-adherent films parts | - surface roughness decreases | - no visible changes | - surface corrosion; - pits formed on surface | - surface corrosion; - pits formed on surface | |
| Nabutan | | | | - uniform surface; - some black holes on surface | - higher surface roughness | | unaffected surface | - surface roughness decreases | | - surface corrosion; - pits formed on surface | - surface corrosion; - pits formed on surface | |
| Iridite NCP | | | | - uniform surface; - some black holes on surface | - relative surface roughness | | unaffected surface | - surface roughness decreases | | - some corrosion on surface after 48 h | - some corrosion on surface after 48 h | |

Table 6 – Results obtained for Al2219 test panels.

| Chemical conversion coating | 'As received' | | | 'As produced' | | | TC | | SS | | TC + SS |
|-----------------------------|---|----------------------------|----------------|---|-------------------------------|--|---|-------------------------------|----------------------|--|--|
| | SEM | Roughness | Resistivity | SEM | Roughness | Resistivity | SEM | Roughness | Resistivity | Visual Analysis | |
| Alodine 1200S | | | | - uniform coating; - typical mud-cracked surface morphology; - black spots on surface | - surface roughness decreases | | - more compact and uniform surface | - surface roughness decreases | | - no evidence of corrosion | - no evidence of corrosion |
| Alodine 5700 | - The remaining particles on surface were secondary phases from the corresponding aluminium alloy | - higher surface roughness | - not measured | - coating peeled-off; - poor adhesion to substrate | - higher surface roughness | - surface electrical resistivity is very similar | complete peel-off of the non-adherent films parts | - surface roughness decreases | - no visible changes | - surface corrosion; - pits formed on surface | - surface corrosion; - pits formed on surface |
| Nabutan | | | | - uniform surface; - some black holes on surface | - higher surface roughness | | unaffected surface | - surface roughness decreases | | - surface corrosion; - pits formed on surface | - surface corrosion; - pits formed on surface |
| Iridite NCP | | | | - uniform surface; - some black holes on surface | - relative surface roughness | | unaffected surface | - surface roughness decreases | | - some corrosion on surface after 48 h | - some corrosion on surface after 48 h |

Table 7 – Results obtained for AI5083 test panels.

| Chemical conversion coating | 'As received' | | | 'As produced' | | | TC | | | SS | TC + SS |
|-----------------------------|---|------------------------------|----------------|--|-------------------------------|--|------------------------------------|-------------------------------|----------------------|---|---|
| | SEM | Roughness | Resistivity | SEM | Roughness | Resistivity | SEM | Roughness | Resistivity | Visual Analysis | Visual Analysis |
| Alodine 1200S | | | | - uniform coating surface; morphology; -black spots on surface | - surface roughness decreases | | - more compact and uniform surface | - surface roughness decreases | | - no evidence of corrosion | - no evidence of corrosion |
| Alodine 5700 | - The remaining particles on surface were secondary phases from the corresponding aluminium alloy | - relative surface roughness | - not measured | - good adhesion to substrate | - higher surface roughness | - surface electrical resistivity is very similar | - more uniform and compact surface | - surface roughness decreases | - no visible changes | - surface corrosion; - pits formed on surface | - surface corrosion; - pits formed on surface |
| Nabutan | | | | - uniform surface; - some black holes on surface | - higher surface roughness | | unaffected surface | - surface roughness decreases | | - surface corrosion; - pits formed on surface | - surface corrosion; - pits formed on surface |
| Iridite NCP | | | | - uniform surface; - some black holes on surface | - relative surface roughness | | unaffected surface | - surface roughness decreases | | - some corrosion on surface after 48 h | - some corrosion on surface after 48 h |

4 Conclusions

- Chemical cleaning of the as-received sheet samples in Novaclean A186 has been seen to decrease the surface roughness of all alloys (Al7075, Al2219 and Al5083).
- The coating supplier recommended processes were applied. Only Alodine 1200S was observed to be defect-free after its application. The other coatings contained some defects. For Alodine 5700, even immersion time variations did not exclude defects (except for the 30-second immersion).
- Only the Alodine 1200S samples (for all alloys) survived thermal cycling; the other conversion coatings were seen to partially spall-off.
- The electrical resistivities of all samples were very similar, even after thermal cycling.
- Only the Alodine 1200S samples (for all alloys) can be considered to have survived the salt spray test. The other coatings (Alodine 5700, Iridite NCP and Nabutan STI/310) did not provide adequate corrosion protection.
- For Al5083, chromium free coatings seem to have promising corrosion behaviour.
- Only Alodine 1200S provided a compact finish. The other coatings tended to spall-off and are considered to be a severe source for contamination in any given spacecraft application.
- It is recommended that corrosion protection schemes for ESA spacecraft continue to utilise Alodine 1200S, as the other (hexavalent chromium-free) coatings did not provide suitable protection.

5 References

- [1] Official Journal of the European Union, L 37/19 from 13.02.2003
- [2] <http://aluminium.matter.org.uk/aluselect>
- [3] http://esmat.esa.int/Services/Preferred_Lists/Materials_Lists/materials_lists_0.html
- [4] NCAP Phase I Report "Non-Chromate aluminum pretreatments"; USA, August (2003)
- [5] ASST 2006 – "Aluminium Surface Science and Technology", 4th Int. Symp, Beaune, France, May (2006)
- [6] Y. Sepulveda, C.M. Rangel, M.A. Paez, P. Skeldon, and G.E. Tompson, "ASST 2006 – Aluminium Surface Science and Technology", Abstract 76, 4th Int. Symp. (2006)
- [7] A.E. Hughes, M. Forsyth, N. Dubrule, T. Markley, B. Hinton, and S.A. Furman, "ASST 2006 – Aluminium Surface Science and Technology"; Abstract 55, 4th Int. Symp. (2006)
- [8] D. Raps, T. Hack, E. Kock and M. Beneke, "ASST 2006 – Aluminium Surface Science and Technology", Abstract 148, 4th Int. Symp. (2006)
- [9] *Alodine 1200S - Technical Process Bulletin*, HENKEL Surface Technologies (1999)
- [10] *Alodine 5200/5700 - Technical Process Bulletin*, HENKEL Surface Technologies (2006)
- [11] *SurTec 650 - Chromital TCP, Technical Process Bulletin*, CST – SurTec Inc. (2006)
- [12] *Nabutan STI/310 - Technical Process Bulletin*, NABU-Oberflächentechnik GmBH (1997)
- [13] *Iridite NCP - Technical Process Bulletin*, MacDermid Industrial Solutions (2005)
- [14] *Iridite NCP - Surface Conditioning Systems*, Information supplied by MacDermid Industrial Solutions (2005)
- [15] M.W. Kendig and R.G. Buchheit, "Corrosion Inhibition of Aluminum and Aluminum Alloys by Soluble Chromates, Chromate Coatings, and Chromate-Free Coatings", Critical Review of Corrosion Science and Engineering, *Corrosion*, **59** (2003) 379
- [16] P. Campestrini, E.P.M. van Westing and J. H. W. de Wit, "Influence of surface preparation on performance of chromate conversion coatings on Alclad 2024 aluminium alloy: Part I: Nucleation and growth", *Electrochimica Acta*, **46** (2001) 2553
- [17] P. Campestrini, E.P.M. van Westing and J.H.W. de Wit, "Influence of surface preparation on performance of chromate conversion coatings on Alclad 2024 aluminium alloy: Part II: EIS investigation", *Electrochimica Acta*, **46** (2001) 2631
- [18] J.R. Waldrop and M.W. Kendig, "Nucleation of chromate conversion coating on aluminum 2024-T3 investigated by Atomic Force Microscopy", *J. Electrochem. Soc.*, **145** (1998) L11-L13

- [19] G.M. Brown and K.J. Kobayashi, "Nucleation and growth of a chromate conversion coating on aluminum alloy AA 2024-T3", *J. Electrochem. Soc.*, **148** (2001) B457-B466
- [20] X. Sun, R. Li, K.C. Wong and A.R. Mitchell, "Surface effects in chromate conversion coatings on 2024-T3 aluminium alloy", *Journal of Materials Science*, **36** (2001) 3215
- [21] G.M. Treacy and G.D. Wilcox, "Surface analytical study of the corrosion behaviour of chromate passivated Al 2014 A T-6 during salt fog exposure", *Applied Surface Science*, **157** (2000) 7
- [22] O. Lunder, J.C. Walmsley, P. Mack and K. Nisancioglu, "Formation and characterisation of a chromate conversion coating on AA6060 aluminium", *Corrosion Sci.*, **47** (2005) 1604
- [23] Qingjiang Meng and G. S. Frankel, "Characterization of chromate conversion coating on AA7075-T6 aluminum alloy", *Surf. Interface Anal.*, **36** (2004) 30
- [24] J.M.C. Mol, A.E. Hughes, B.R.W. Hinton and S. van der Zwaag, "A morphological study of filiform corrosive attack on chromated and alkaline-cleaned AA2024-T351 aluminium alloy", *Corrosion Sci.*, **46** (2004) 1201
- [25] G.P. Bierwagen, R. Twite, G. Chen and D.E. Tallman, "Atomic force microscopy, scanning electron microscopy and electrochemical characterization of Al alloys, conversion coatings, and primers used for aircraft", *Progress in Organic Coatings*, **32** (1997) 25
- [26] L. Fedrizzi, A. Bianchi, F. Deflorian, S. Rossi and P.L. Bonora, "Effect of chemical cleaning on the corrosion behaviour of painted aluminium alloys", *Electrochimica Acta*, **47** (2002) 2159
- [27] J. Zhao, L. Xia, A. Sehgal, D. Lu, R. L. McCreery and G. S. Frankel, "Effects of chromate and chromate conversion coatings on corrosion of aluminum alloy 2024-T3", *Surface and Coatings Technology*, **140** (2001) 51
- [28] J.W. Bibber, "An overview of non-hexavalent chromium conversion coatings - Part I: aluminum and its alloys", *Metal Finishing*, **99** (2001) 15
- [29] B.R.W. Hinton, "Corrosion inhibition with rare earth metal salts", *J. Alloys Compounds*, **180** (1992) 15
- [30] M. Bethencourt, F.J. Botana, M.J. Cano and M. Marcos, "Advanced generation of green conversion coatings for aluminium alloys", *Applied Surface Science*, **238** (2004) 278
- [31] D.R. Arnott, N.E. Ryan, B.R.W. Hinton, B.A. Sexton and A.E. Hughes, "Auger and XPS studies of cerium corrosion inhibition on 7075 aluminum alloy", *Applications of Surface Science*, **22-23** (1985) 236
- [32] W.G. Fahrenholtz, M.J. O'Keefe, H. Zhou and J.T. Grant, "Characterization of cerium-based conversion coatings for corrosion protection of aluminum alloys", *Surface and Coatings Techn.*, **155** (2002) 208
- [33] B.F. Rivera, B.Y. Johnson, M.J. O'Keefe and W.G. Fahrenholtz, "Deposition and characterization of cerium oxide conversion coatings on aluminum alloy 7075-T6", *Surface and Coatings Techn.*, **176** (2004) 349

- [34] A. Decroly and J.-P. Petitjean, "Study of the deposition of cerium oxide by conversion on to aluminium alloys", *Surface and Coatings Tech.*, **194** (2005) 1
- [35] J. Hu, X.H. Zhao, S.W. Tang and M.R. Sun, "Corrosion protection of aluminum borate whisker reinforced AA6061 composite by cerium oxide-based conversion coating", *Surface and Coatings Techn.*, **201** (2006) 3814
- [36] J. Hu, X.H. Zhao, S.W. Tang, W.C. Ren and Z.Y. Zhang, "Corrosion resistance of cerium-based conversion coatings on alumina borate whisker reinforced AA6061 composite", *Applied Surface Science*, **253** (2007) 8879
- [37] L.E.M. Palomino, I.V. Aoki and H.G. de Melo, "Microstructural and electrochemical characterization of Ce conversion layers formed on Al alloy 2024-T3 covered with Cu-rich smut", *Electrochimica Acta*, **51** (2006) 5943
- [38] L.E.M. Palomino, P.H. Suegama, I.V. Aoki, Z. Pászti and H.G. de Melo, "Investigation of the corrosion behaviour of a bilayer cerium-silane pre-treatment on Al 2024-T3 in 0.1 M NaCl", *Electrochimica Acta*, **52** (2007) 7496
- [39] A.E. Hughes, J.M.C. Mol, B.R.W. Hinton and S. van der Zwaag, "A morphological study of filiform corrosive attack on cerated AA2024-T351 aluminium alloy", *Corrosion Sci.*, **47** (2005) 107
- [40] H. Guan and R.G. Buchheit, "Corrosion Protection of Aluminum Alloy 2014-T3 by Vanadate Conversion Coatings", *Corrosion Science Section*, Corrosion (2004)
- [41] M. Khobaib, L.B. Reynolds and M.S. Donley, "A comparative evaluation of corrosion protection of sol-gel based coatings systems", *Surface and Coatings Tech.*, **140** (2001) 16
- [42] X.F. Yang, D.E. Tallman, V.J. Gelling, G.P. Bierwagen, L.S. Kasten and J. Berg, "Use of a sol-gel conversion coating for aluminum corrosion protection", *Surface and Coatings Tech.*, **140** (2001) 44
- [43] R.L. Parkhill, E.T. Knobbe and M.S. Donley, "Application and evaluation of environmentally compliant spray-coated ormosil films as corrosion resistant treatments for aluminum 2024-T3", *Progress in Organic Coatings*, **41** (2001) 261
- [44] M. Zhao, S. Wu, P. An, J. Luo, Y. Fukuda and H. Nakae, "A chromium-free conversion coating of magnesium alloy by a phosphate-permanganate solution", *Surface and Coatings Techn.*, **200** (2006) 5407
- [45] M. Zhao, S. Wu, P. An and J. Luo, Y. Fukuda and H. Nakae, "Microstructure and corrosion resistance of a chromium-free multi-elements complex coating on AZ91D magnesium alloy", *Materials Chemistry and Physics*, **99** (2006) 54
- [46] M. Zhao, S. Wu, P. An, Y. Fukuda and H. Nakae, "Growth of multi-elements complex coating on AZ91D magnesium alloy through conversion treatment", *J. Alloys and Compounds*, **427** (2007) 310
- [47] M. Zhao, S. Wu, P. An and J. Luo, "Study on the deterioration process of a chromium-free conversion coating on AZ91D magnesium alloy in NaCl solution", *Applied Surface Science*, **253** (2006) 468

- [48] H. Umehara, M. Takaya and S. Terauchi, "Chrome-free surface treatments for magnesium alloy", *Surface and Coatings Tech.*, **169** (2003) 666
- [49] L.-H. Chiu, C.-C. Chen and C.-F. Yang, "Improvement of corrosion properties in an aluminum-sprayed AZ31 magnesium alloy by a post-hot pressing and anodizing treatment", *Surface & Coatings Technology*, **191** (2005) 181
- [50] M.F. Montemor, A.M. Simões, M.G.S. Ferreira and M.J. Carmezim, "Composition and corrosion resistance of cerium conversion films on the AZ31 magnesium alloy and its relation to the salt anion", *Applied Surface Science* (submitted 2007)
- [51] M.F. Montemor, A.M. Simões and M.J. Carmezim, "Characterization of rare-earth conversion films formed on the AZ31 magnesium alloy and its relation with corrosion protection", *Applied Surface Science*, **253** (2007) 6922
- [52] D. Battocchi, A.M. Simões, D.E. Tallman, G.P. Bierwagen, "Comparison of testing solutions on the protection of Al-alloys using a Mg-rich primer", *Corrosion Science*, **48** (2006) 2226
- [53] Surface roughness tester – User's Manual by Mitutoyo (1999)
- [54] <http://trs-new.jpl.nasa.gov/dspace/bitstream/2014/18241/1/99-1710.pdf>
- [55] http://www.efcweb.org/efcweb_media
- [56] ASTM B117/07 – Standard Practice for Operating Salt Spray (Fog) Apparatus (2007)